

Formation of ophiolite-bearing tectono-sedimentary mélanges in accretionary wedges by gravity driven submarine erosion: Insights from analog models and case studies

^{1,2}Malavieille Jacques, ³Molli Giancarlo, ¹Genti Manon, ^{1,2}Dominguez Stephane, ⁴Beysac Olivier, ^{1,2}Taboada Alfredo, ⁴Vitale-Brovarone Alberto, ^{5,2}Lu Chia-Yu, ⁵Chen Chih-Tung

¹ Université de Montpellier, Géosciences Montpellier, Place E. Bataillon, 34095 Montpellier cedex 5, France

² LIA D3E, C.N.R.S.-M.O.S.T. France-Taiwan International Laboratory

³ Università di Pisa, Dipartimento di Scienze della Terra, Via S.Maria, 53, 56126 Pisa, Italy

⁴ Sorbonne Universités - UPMC Univ Paris 06, Institut de Minéralogie, de Physique des Matériaux, et de Cosmochimie (IMPMC), UMR CNRS 7590, 4 Place Jussieu, F-75005 Paris, France

⁵ National Taiwan University, Department of Geosciences, Taipei, Taiwan.

Abstract

Orogenic wedges locally present chaotic tectonostratigraphic units that contain exotic blocks of various size, origin, age and lithology, embedded in a sedimentary matrix. The occurrence of ophiolitic blocks, sometimes huge, in such “mélanges” raises questions on i) the mechanisms responsible for the incorporation of oceanic basement rocks into an accretionary wedge and ii) the mechanisms allowing exhumation and redeposition of these exotic elements in “mélanges” during wedge growth.

To address these questions, we present the results of a series of analog experiments performed to characterize the processes and parameters responsible for accretion, exhumation and tectonosedimentary reworking of oceanic basement lithosphere fragments in an accretionary wedge.

The experimental setup is designed to simulate the interaction between tectonics, erosion and sedimentation. Different configurations are applied to study the impact of various parameters, such as irregular oceanic floor due to structural inheritance, or the presence of layers with contrasted rheology that can affect deformation partitioning in the wedge (frontal accretion vs basal accretion) influencing its growth. Image correlation technique allows extracting instantaneous velocity field, and particles tracking. By retrieving the particle paths determined from models, the pressure-temperature path of mélangé units or elementary blocks can be discussed. The experimental results are then compared with observations from ophiolite-bearing mélanges in Taiwan (Lichi and Kenting mélanges) and RSCM Thermometry data on rocks of the Casanova mélange (northern Apennines). In the latter case study, peak metamorphic temperature was determined by RSCM thermometry. Based on all these observations, it is proposed that the tectonic evolution of the retroside of doubly vergent accretionary wedges is mainly controlled by backthrusting and backfolding. The retro wedge is actually characterized by steep slopes that are prone to gravitational instabilities. It triggers submarine landslides inducing huge mass transfers. This erosion combined with backthrusting could favour exhumation of the ophiolitic fragments formerly accreted at the base of the wedge along the rough seafloor-sediments interface. Such an exhumed material can be reworked and deposited as debris-flows in proximal basins located at the foot of the retrowedge slope forming a tectono-sedimentary mélange. These syntectonic basins are continuously deformed and involved in prograding backthrusting-induced deformation.

Keywords: tectono-sedimentary mélanges; ophiolites; analog modeling; RSCM thermometry; submarine erosion; Casanova mélange, Apennines; Kenting & Lichi mélanges, Taiwan

Introduction

Many mountain belts show tectono-stratigraphic mélanges made up by rock-types and units of

different ages and nature (e.g., Hsü, 1965; Raymond, 1984; Cowan, 1985; Orange and Underwood, 1995)). The interpretation of these *mélange* complexes raises questions about their origin, mechanisms of formation and geodynamic significance. In turn, their internal structure and rock-assemblages contain valuable information regarding orogenic processes and corresponding geodynamic setting. Many studies document a complete history including *mélanges* evolution throughout time (among others; Silver and Beutner, 1980; Page and Suppe, 1981; Sakai, 1981; Cloos, 1984; Raymond, 1984; Saleeby, 1984; Yilmaz and Maxwell, 1984; Cowan, 1985; Moore and Byrne, 1987; Barber and Brown, 1988; Cloos and Shreve, 1988; Bettelli and Panini, 1989; Brandon, 1989; Pollock, 1989; Talbot and von Brunn, 1989; Kimura and Mukai, 1991; Orr et al., 1991; Roure et al., 1991; Jeanbourquin et al., 1992; Labaume, 1992; Matsuda and Ogawa, 1993; Needham, 1995; Steen and Andreson, 1997; Meschede et al., 1999; Bettelli and Vannucchi, 2003; Alonso et al., 2006; Huang et al., 2008; Meneghini et al., 2009; Osozawa et al., 2009; Ghikas et al., 2010; Festa et al., 2010; 2014; Wakabayashi, 2011b; Codegone et al., 2012; Hernaiz Huerta et al., 2012; Ogata et al., 2012; Hajna et al., 2014; Ogawa et al., 2014; Alonso et al., 2015; Platt, 2015; Ukar and Cloos, 2015), but many questions remain. In a review paper, Festa et al. (2010) classified the different kinds of *mélanges* as a function of their tectonic setting (extensional, strike-slip and compressional of various types). Three main *mélange*-forming processes are considered within the different settings: tectonics, sedimentation and diapirism, with gravity playing a key and general role during their final emplacement (e.g., Lucente and Pini, 2003; Alonso et al., 2006).

Many tectono-sedimentary *mélanges* are related to oceanic accretionary wedges developed in convergent subduction settings. Some of them show ophiolite blocks sometimes of kilometric size, embedded in an original sedimentary matrix (Franciscan *mélange* in California, e.g., Hsü, 1968; Wakabayashi, 2011a, Lichi *mélange* in Taiwan, Hsu, 1956; Page and Suppe, 1981; Casanova *mélange* in the northern Apennines, Elter et al., 1991, etc.). Among other characters, the presence of ophiolites raises the question of the mechanisms responsible for the incorporation and exhumation of fragments of oceanic lithosphere within an accretionary wedge- and/or a mountain chain-related

sedimentary basin.

On a global scale different stages of orogenic wedge development can be observed and studied (from the stage of intraoceanic accretionary wedge to that of a mature mountain belt). Nevertheless, it is very difficult in natural examples to track their complete tectonic and geodynamic history and mélangé-evolution throughout time from the inception of subduction and during wedge growth. In this paper, scaling the length and time scales, we use an experimental approach to obtain complete time-tracking of early prism evolution and mélangé formation. Our approach, introduces natural processes such as erosion and sedimentation coeval with shortening and contractional deformation of the prism (e.g. Gravelleau et al. 2012). Detailed geometric, kinematic and mechanical analyses are therefore possible to test the role played by different parameters and boundary conditions in the formation of ophiolite-bearing tectono-sedimentary mélanges related to submarine accretionary prisms. This experimental approach has been successfully applied to simulate formation and deformation of tectono-sedimentary mélanges in the frontal part of accretionary wedges in relation with seamounts or ridges subduction (Lallemand et al., 1992; Gutscher et al., 1998a; Dominguez et al., 2000). It has been shown that a strong deformation affects the frontal part of the wedge and that disrupted sequences (mélanges) can be dragged at depth and then incorporated at the base of the prism (Dominguez et al., 1998a, 1998b, 2000). In this study, we consider that a large part of the accreted material is constituted by rocks snatched from the irregular oceanic floor (ophiolitic debris or slices) mixed with dismembered sedimentary sequences and dragged to the deep part of the accretionary prism through a subduction channel (e.g., Von Huene et al., 2004). Assessing the fate to these rocks after burial in the core of the wedge is the main objective of this study. The mechanisms responsible for the exhumation of these deeply buried fragments, and then the tectono-sedimentary processes allowing reworking and deposition in orogenic basins as mélanges are discussed. Our experiments allow a detailed parametric study of the processes responsible for material transfer in different wedge settings, taking into account the boundary conditions of a subduction zone, the main mechanical parameters involved for wedge development (rheology of the

incoming sequence, basal friction, role of décollements) and the impact of surface processes (erosion-sedimentation). Results of the experimental study are then compared to two natural case-studies for which the geology is well known, the ophiolite-bearing mélanges of Casanova in the northern Apennines, and the Lichi and Kenting mélanges of Taiwan. A study of peak metamorphic temperature using thermometry based on Raman spectroscopy of carbonaceous material (RSCM) on rocks from the Casanova mélange bring important information on the pathways followed by sediments and ophiolitic debris during burial, subsequent exhumation and redeposition in the retrowedge basin. Finally, we propose an integrative model for the formation of mélanges in accretionary wedge settings.

Experimental setup and procedure

The experimental setup simulates the basic geometry, kinematics and the main mechanisms of a subduction zone where lower plate crustal materials sink beneath an upper plate (Fig. 1). This domain of the upper-plate located above the subduction interface corresponds in the experiments to the arc-forearc upper-crust basement simulated by a rigid backstop. The backstop upper-plate presents a low angle dip and the friction on top of its surface can be adapted from high to low. This geometry has been chosen by analogy to natural upper-plate settings where a low dipping basement represents the rigid part of the subduction upper-plate, as in the forearc of Taiwan for example (see profiles in Lin et al., 2009). In order to simulate a doubly vergent prism (Malavieille, 1984; Gutscher et al., 1998b; Hoth et al., 2006), the following conditions have been fulfilled: the system is not in a regime of dominant tectonic erosion (the term “tectonic erosion“ is used in the sense of Lallemand et al., 1994, when enough material is available for accretion); the presence of a velocity discontinuity (S-point Fig. 1b) and available space on top of the backstop (rightward of the S-point). A no material output boundary condition has been chosen as it represents an end member among two extreme behaviours of active margins in terms of mass flux balance, and it corresponds to the

situation where accretion is maximum (Gutscher et al., 1998a). All experiments are performed under normal gravity field in a classical sandbox (see Malavieille, 1984; Konstantinovskaia & Malavieille, 2005; 2011), adapted to allow large shortening (over 200 cm) and presenting a flexure of the basal plate, simulating the curvature of a subducting plate. The sandbox (Fig. 1a) is 10 cm wide and 300 cm long. Sidewall glasses allow a continuous and non-destructive 2D observation of experiments. To make friction along the sidewalls negligible, the glasses are coated with a special product (Rain-X glass water repellent). At the base of the box, a thin plastic strip (dacron cloth) exits from the device through a thin slot located at the tip of the rigid buttress. It is pulled by a computer controlled stepper motor. Analog materials materializing the trench fill sediments and the upper crust rocks of the oceanic lower plate (green layer = ophiolite-bearing sediments) are deposited onto the plastic strip and are dragged toward the upper-plate backstop. As they cannot exit from the device (no output), they are accreted forming an accretionary prism. Different basal frictions have been applied to test the impact of this parameter on wedge dynamics and address important questions. The questions addressed here are: What structural evolution characterizes a high friction wedge compared to a low friction one? What is the impact of upper-plate friction on the evolution of the retrowedge submitted or not to surface erosion? In that purpose, friction at the base of the model materials can be adjusted using different procedures. To obtain a high basal friction ($\mu_b \approx 0.5$) between the basal strip and the analog material, a thin layer of sand grains is glued on top of the plastic strip, leading to a very rough surface. The same procedures have been applied to the surface of the smooth PVC plate simulating a rigid upper-plate backstop. The basal friction has been measured in our modeling laboratory using a shear box that we specifically designed to characterize the analogue materials used in various experiments (see a view of the shear box in Graveleau et al., 2011, Figure 5). It also allows for measuring the friction between two different medium (our basal friction), for example, between our Dacron cloth and a granular material. In the described experiments, the “high” basal friction is around 0.6, “low” basal friction

is around 0.35. A very low basal friction ($\mu_b \approx 0.2$) is obtained by covering the top of the smooth plastic strip with glass microbeads.

According to the critical wedge theory (Davis et al., 1983; Dahlen et al., 1984; Dahlen, 1984), the strength of the basal décollement influences the dipping of the main thrusts and backthrusts and the surface slope angle of a wedge that satisfies the yield conditions (Fig. 1b).

Three different materials are used in the models (Table 1). 1) Aeolian sand, with a density of 1690 kg/m³, with well rounded grains less than 300 μ m in size, a coefficient of internal friction (μ_0) of 0.57 and a cohesion (C) of ≈ 20 Pa. It composes the upper plate protowedge and a large part of lower plate layers. 2) Layers of glass microbeads are used to model weak layers in the sandcake (décollements). Diameter is $\approx 100 - 200 \mu$ m, and the perfect roundness of the grains yields a smaller coefficient of internal friction ($\mu_0 = 0.44$) and a negligible cohesion. 3) Aeolian sand mixed with silica powder with a strong cohesion (C) of ≈ 150 Pa, forms green layer at the base of the multilayer. This latter material simulates rocks from the rough basement floor of the oceanic crust and covering trench sediments that are prone to be offscraped and accreted at the base of the accretionary prism through the subduction channel.

Aeolian sand, glass microbeads and powders are commonly used in physical modeling studies as analogs of upper crustal rocks with brittle behavior. The scaling factor between their mechanical properties and those of the natural prototype is around 10^5 (Krantz, 1991; Schellart, 2000; Lohrman et al., 2003). The same 10^5 scaling factor is therefore used for model dimensions (1 cm \approx 1 km), in order to satisfy the fundamental scaling theory for analog modeling (Hubbert, 1937, 1951; Horsfield, 1977; Ramberg, 1981; Davy and Cobbold, 1991; Graveleau et al., 2011).

Nine experiments have been run to test several first order parameters. Among them, seven were chosen to describe the main results of our study and characterize first order processes involved in mélange formation (Figs. 2 and 3). We assume that the main process responsible for surface erosion in submarine accretionary prisms is caused by gravitational instability of unstable wedge slopes.

Thus, in some of the experiments, surface erosion and sedimentation are applied in the rear part of the wedge, following the procedure described here below. First, an initial shortening without surface erosion is applied to the models, allowing the development of a wedge shaped topographic relief. This first step of tectonic accretion (e.g., Von Huene et al., 2004) can be considered as the analog of wedge development in a submarine setting when few erosion affects the surface of the wedge slopes. When the critical taper is reached by the growing wedge, sedimentation at the rear of the retroside is performed by sprinkling sand on the low-angle backstop (analog to a subduction upper-plate setting). Then, manually operated erosion of the retrowedge surface is performed with a thin metal plate (the sand being removed using a vacuum cleaner) to maintain the slope at a constant angle. This slope corresponds to the critical taper slope of a dry sand wedge (Davis et al., 1983). Slope angles in experiments are much higher than in natural submarine conditions. Long-term erosion in nature is simulated by a roughly constant erosion rate applied to the models step by step, each 2 cm of convergence. Even when varying the rates of the surface processes, the experimental procedure was based on the assumption that the tectonic development of the model influences the respective rates and location of erosion and sedimentation. In this case, local erosion rates are directly controlled by the activity of thrusts. Erosion of the units was applied in a constant manner, independently of their lithological nature, only as a function of the topographic slope. This is supported by other analogue modelling studies (Hoth et al., 2004; Konstantinovskaia and Malavieille, 2005), and by observations from natural settings where erosion can be positively correlated with slope (e.g., Summerfield and Hulton, 1994; Hooke, 2003). The varying qualitative rates of imposed erosion and sedimentation are indicated for the seven described experiments. Overall the erosion/sedimentation budget (surface fluxes) is not balanced in the sense that more material is removed out of the system than is deposited (output > input). This is equivalent to the natural situation in most forearc basins, where more than half of the incoming sediments can be carried out of the system through submarine canyons into the neighbouring sinks (the subduction trench or back-arc basins, as for instance east of Taiwan).

We place a camera in front of the glass sidewall in order to have a global view of the doubly-vergent prism formed by accretion of analogue material multilayers. We took a picture every 5mm of shortening. Image resolution varies from 333 to 417 microns per pixel depending on the experiment. Images are correlated sequentially to extract the instantaneous velocity field, using an algorithm of sub-pixel correlation (Van Puybroeck et al., 2000). To have a good correlation we mix 1% of dark sand in every layer. Our analysis reveals the prism development kinematics (Fig. 3), for each time we can infer deformation localization of active accretion. Thanks to the integration of all velocity fields we can calculate and highlight particle paths (Fig. 3c).

Experimental results

Hereafter the results of seven chosen experiments are analyzed (Fig. 2). Several experiments present minor differences with the general set up of the Figure 1 that are detailed hereafter.

Experiment 1 (Figs. 2a, 3a), the basal friction is low on the moving sheet and the rigid upper-plate backstop is covered by a thin layer of glass beads allowing a low basal friction. The prism is only build up with sand and it is run without surface erosion and sedimentation (sand is manually removed from the retrowedge slope). The total shortening is of 170 cm. A doubly vergent wedge develops with similar retro and prowedge slope angles (around 10°). No gravitational instability occurs on the retrowedge low-angle slope. We observe that the main backthrust follows the interface between the backstop and the base of the sand model. It enables the development of a wide low-angle retrowedge slope favoured by the low basal friction. The green basal layers ("model ophiolites") are continuously incorporated to the retrowedge overthrusting the backstop, but as no exhumation occurs this setting does not allow it to reach the surface.

Experiment 2 (Figs. 2b, 3b), the basal friction is low on the moving sheet and the friction on the backstop surface is high. A weak layer of glassbeads is located in the middle of the sandcake, 1cm above the green basal layer. It is run without manually operated erosion and sedimentation (see the movie 1 in the supplementary material). The total shortening is of 160 cm. A doubly vergent wedge

develops showing different slope angles with a retrowedge slope (35°) steeper than the prowedge one (7°). During the growth, the steep retrowedge slope exceeds the value of the internal friction angle, triggering spontaneous surface erosion by gravitational collapse of the sand. A subsequent low sedimentation rate occurs at the foot of the retrowedge slope. The newly deposited material is sheared and folded, under the retrowedge backthrust. The basal layers ("model ophiolites") involved in former forethrusts are backthrust on top of the upper-plate, but they never reach the surface (no real exhumation occurs). The décollement layer does not change drastically the behavior of the model wedge, few deformation partitioning occurs. It induces only minor differences in geometry between the thrust units located above and below the décollement layer.

Experiment 3 (Figs. 2c, 3c, 4a), the basal friction is low on the moving sheet and the friction on the backstop surface is high (total shortening of 150 cm). The model is composed of sand only. Surface erosion is performed each 4 cm of shortening and sedimentation each 2 cm. During this experiment a doubly vergent wedge develops with a retrowedge slope (around 19°) steeper than that of the prowedge (around 6°). The retrowedge overlaps the newly deposited material thanks to the backthrust. In the basin, the layering is slightly folded under the backthrust. Retrowedge slope and basin filling are affected by erosion. Green basal layers ("model ophiolites") are lifted thanks to backthrusting but the high sedimentation rate in the basin does not allow a complete exhumation up to the surface and as a consequence, the basin infill does not contain pieces of the green material.

Experiment 4 (Figs. 2d, 3d, 4b), the basal friction is high on both the moving sheet and the backstop (total shortening of 176 cm). The prism is made only of sand material. Surface erosion is performed each 4 cm of shortening and the material removed from the slope is deposited in the basin (see the movie 2 in the additional material). A doubly vergent wedge with a steep slope retrowedge (28°) develops. At the beginning of the experiment, during initial filling of the trench, a low dip angle backthrust develops along the surface of the backstop plate. Then backthrusting activity migrates on a newly formed major backthrust whose dip angle is higher than previous and that remains continuously active during shortening. The retrowedge overlaps and deforms both the

early formed tectonic unit and the newly deposited material of the syntectonic basin. Due to continuous erosion, the green basal layer (“model ophiolites”) involved in former forethrusts, is progressively exhumed and reaches the surface of the retrowedge slope after 136 cm of shortening. Concomittantly, backthrust units are reworked through surface erosion and redeposited downslope in the basin.

Experiment 5 (Figs. 2e, 3e), the basal friction is high on both the moving sheet and the back-stop (total shortening of 180 cm). A weak layer of glassbeads (“décollement”) is located in the sandcake one centimeter above the basal plate, on top of the cohesive green basal layer (“model ophiolites”). The model is run with retrowedge surface erosion applied each 4 cm of shortening, the material removed from the slope is deposited in the basin. A doubly vergent wedge develops with a double slope prowedge and a steep slope retrowedge (27°). The location of the weak layer, deeper than in experiment 2 (compare Fig. 3b and Fig. 3e), favours basal accretion. Deformation partitioning is maximum and it allows a complete underplating of the tectonic units located below the décollement, ie. the green basal layer (“model ophiolites”). The part of the prowedge located above the domain of basal accretion presents a 12° angle of slope higher than the slope of the frontal part (3°) that is controlled by the low friction layer. The green material involved in the accreted duplexes is strongly deformed and sheared. Then, from 80 cm to the end of shortening a large amount of underplated “model ophiolites” reaches the retrowedge slope surface allowing erosion and deposition of the exhumed material in the basin (Fig. 5). The deposited material is continuously sheared and deformed when involved under the main backthrust.

Experiment 6 (Figs. 2f, 3f), the basal friction is low on both the moving sheet and the backstop (total shortening of 164 cm). The model is run with retrowedge surface erosion and sedimentation in the basin. Erosion is applied each time a new tectonic unit appears in front of the forewedge. At the same time, an equivalent volume of eroded material is deposited in the basin, involving half a volume of sand and half a volume of glass microbeads. The aim of such a setting was to facilitate backthrusting and to enhance deformation of basin material. We observe the development of a

doubly vergent wedge with a steep retrowedge slope (29°). Erosion of the retrowedge slightly modifies forewedge growth. The retrowedge overlaps the newly deposited material thanks to a major backthrust whose dip angle increases with basin infilling. At 60 cm of shortening, the green basal layer ("model ophiolites") involved in former forethrust units is exhumed, reaching the surface in the retrowedge, and parts of it are deposited in the basin, until the end of the experiment. Layering in the basin is gently deformed under the backthrust at the vicinity of the contact, locally involving shearing and subsequent folding and overturning of the layers.

Experiment 7 (Figs. 2g, 3g), represents the case of an overhanging backstop upper-plate simulating in nature an uplifted part of continental or volcanic arc upper-plate basement. In the model, the backstop is made with a cohesive granular material (mix sand-powder) which strength is higher than that of pure sand but that can be deformed during wedge growth. Evolution of the forewedge is classic, but as expected, no major backthrusting occurs preventing the development of a clear retrowedge side. Although deformation (diffuse backthrusting and uplift) occurs in the overhanging backstop, wedge materials are never backthrusted on top of it. As a consequence, the green basal layers ("model ophiolites") never reach the surface. In an equivalent natural setting, one can expect clastic deposits resulting from the erosion of the uplifted upper-plate, continental or oceanic depending on the nature of its basement.

Interpretation of experimental results

Analog models allow a dynamic view of tectonic and sedimentary processes related to accretionary wedge development. Results of experiments suggest that specific settings and boundary conditions are required to develop tectono-sedimentary mélanges in orogenic wedges. As our study focuses on the behaviour of doubly vergent accretionary wedges submitted to retrowedge gravity driven submarine erosion, insights from models will be compared to case studies chosen in appropriate tectonic settings.

A general observation is that friction parameters control the dip slope of the wedges. High frictions

produce high slope angles, low frictions low-angles (e.g., Mulugeta, 1988). Angles of retrowedge slopes are generally higher than forewedge ones favouring erosion induced by gravitational processes (Fig. 1b). This justifies why in our experiments the retrowedge part of the prism with a high basal friction backstop has been submitted to imposed surface erosion. Basal accretion and underplating promote accretion of deep layers in the core of the wedge (e.g. Malavieille, 2010) and then subsequent exhumation through backthrusting and material removal (erosion) in the retrowedge slope (e.g. Exp. 5, Figs. 2d, 3d). A rigid backstop with a low friction surface promotes tectonic transport at the rear of the prism. The displacement of the accreted basal layer is larger for low than for high friction. However, a low friction rigid backstop creates a low-angle retrowedge slope, too low to induce high erosion rates. Significant erosion of retrowedge material and its deposition in proximal basins associated with a low sedimentation rate (low erosion/sedimentation ratio) yield favourable conditions to exhume deep materials. Once basal layers (“model ophiolites”) have reached the surface of the retrowedge, they are likely reworked in the basin as tectono-sedimentary mélanges through gravitational processes (e.g., Hampton et al., 1996; Alonso et al., 2006; Harders et al., 2011). Exhumation of deep layers is favored by backthrusting and surface erosion of the steep retrowedge slope. Analysis of particle paths (see an example in Figure 6) shows that materials from the basal layers of the wedges are exhumed and can reach the surface following a concave pathway across the accretionary wedge that is controlled by backthrusting. Erosion and the behaviour of the analogue material (internal friction angle) control the steepness of the main backthrust and subsequent exhumation of the basal layers (ophiolites) through the retrowedge.

To summarize, insights from our experiments (see the two movies given as supplementary material) suggest that the development of tectono-sedimentary mélanges with ophiolites requires major backthrusting, ophiolites basal accretion and exhumation at the rear of the prism, steep retrowedge slope favouring surface erosion, reworking and deposition in proximal basin. The tectonic evolution of a doubly vergent accretionary wedge is therefore mainly controlled by backthrusting and surface processes (erosion and sedimentation) acting in the retrowedge.

Natural case studies

Block-in matrix mélanges have been variously interpreted as deformed olistostromes or as subduction channel flow mélanges (e.g., Festa et al., 2010; Platt, 2015). A wide literature mainly based on observations in the Franciscan mélanges of California (USA) gives constraints on mélanges formation processes based on the different metamorphic gaps documented between blocks and the matrix (among others, see Cloos 1982 ; Raymond, 1984 ; Cowan, 1985 ; Festa et al., 2012 ; Ukar and Cloos, 2015 and reference therein). It suggests that the highest metamorphic peak of blocks with respect to the matrix constrains the melange formation to tectonic processes occurring in a subduction channel (e.g., Ukar, 2012). However, other studies (see Wakabayashi, 2011 ; Wakabayashi, 2015 ; Platt, 2015) , interpreted these different peaks of metamorphism as resulting from complex processes involving multiple burial-exhumation cycles, subduction erosion and gravitational reworking.

Hereafter are reported the main geological characters of the well studied Casanova mélange in the northern Apennines and the Taiwan mélanges, all located in convergent geodynamic settings. These two settings offer a past subduction zone involving a wide accretionary prism during closure of the alpine Tethys for the North Apennines case and a still active subduction involving the Manila accretionary prism in the arc-continent collision process for the Taiwan case. The ophiolite-bearing Casanova and Taiwan mélanges, have been previously analyzed and compared by Page (1978) mainly to discuss the setting and to assess the tectonic history of the Franciscan mélange in California. Many studies have followed dealing on the formation of mélanges from different origins and settings (see the non exhaustive reference list given in the introduction), which outline that no consensus exists on their significance. Here below, the two Casanova and Taiwan case studies mélanges are analyzed in the frame of their well known geological setting, using geological data, insights from experimental models and complementary data from a RSCM thermometry analysis.

Casanova mélange (Italy): The Casanova mélange (Naylor, 1982), also known as M.Penna-Casanova Complex by Elter et al., (1991), is well exposed in the northwest part of the northern Apennines (Fig. 7a,b), between La Spezia, Genova and Piacenza with the type-area framed by the Aveto Valley (south-east) and the Trebbia valley (west north-west) (Cerrina Feroni et al., 2002, Emilia Romagna geological map).

The northern Apennines segment shares with the western Alps the Late Cretaceous-Middle Eocene geological history. It is characterized by an eastward intraoceanic subduction of the Ligurian Jurassic ocean (Boccaletti et al., 1971; Elter, 1997; Carminati and Doglioni, 2012) inducing the formation of a doubly vergent accretionary wedge (Fig. 7c). After subduction reversal in the Middle-Late Eocene the former retroside of the Alpine prism was partially reworked as the backstop of the Oligocene-onward Apenninic prism. The development of the new prism is related to the westward subduction of relict of Ligurian Tethys oceanic basement and distal Adria continental margin (Elter, 1997; Del Castello et al., 2005; Molli and Malavieille, 2010). The Oligocene-Miocene subduction of the Adria plate was associated with a rear-wedge (Liguro-Provencal) and then intra-wedge (Tyrrheninan) extension in the wake of its retreating slab (Doglioni et al., 1998; Jolivet et al., 1998; Molli, 2008; Carminati and Doglioni, 2012; Malavieille and Molli, 2014), a tectonic frame still active today (e.g. Bennett et al., 2012).

In the Northwest Apennines the Ligurian units are considered as the relict of a former Late Cretaceous - Middle Eocene intraoceanic accretionary wedge (Principi and Treves, 1985; Elter, 1997; Marroni and Pandolfi, 1996; Daniele and Plesi, 2000; Bettelli and Vannucchi, 2002; Molli, 2008; Remitti et al., 2011). The so-called Internal Ligurian units (Elter, 1975) are formed by ophiolites and an Upper Jurassic to Lower Cretaceous sedimentary cover rocks (Cherts, Calpionella limestone and Palombini shales) associated with Upper Cretaceous–Paleocene siliciclastic turbiditic sequences. The Internal Ligurian units are thrust over the External Ligurian Units distinguishable by the presence of the typical Late Cretaceous calcareous dominant sequences (the Helminthoid

Flysch) associated with complexes or pre-flysch formations called ‘basal complexes’ (Marroni et al., 1998; Molli, 2008). We will focus hereafter on the Casanova mélangé (Fig. 8a,b). It consists of variable amounts of mono- and polymict pebbly sandstones and mudstones, with intercalations of coarse- to fine grained lithoarenites. The mélangé includes huge (up to plurihectometer-scale), slide-blocks (“olistoliths”) of mantle ultramafics, gabbros and basalts as well as fragments of supraophiolitic pelagic sedimentary sequences (Palombini shales, Calpionella limestones and Cherts) (Fig. 8b). We observe volumetrically subordinate mafic and felsic granulite as well as Hercynian granitoids interpreted as relicts of the formerly highly thinned Adria continental margin and Ocean Continent Transition (Elter et al., 1991; Molli, 1996; Marroni et al., 1998; Marroni et al., 2002). The Casanova Complex generally grades upward to Upper Campanian-Maastrichtian Helminthoid Flysch, represented by a thick, monotonous sequence of calcareous-turbidites (Marroni et al., 1998; Argnani et al., 2004). The Casanova complex in the type area is exposed in the inverted limb of a large kilometer-scale recumbent fold (Elter, 1975; Elter et al., 1991; Marroni et al., 1998) developed in very low grade metamorphic conditions (Molli et al., 1992). Figure 8 shows schematically the main structural features of the Casanova mélangé as well as its tectonic position between the overlying and underlying units.

A thermometry study was performed to characterize the peak metamorphism of the Casanova mélangé and its overlying units. Organic matter present in rocks is gradually transformed into graphitic carbonaceous material during regional metamorphic processes. This progressive graphitization process can be used for the estimation of peak temperature reached by the studied sample (Beysac et al., 2002). Moreover, graphitization is an irreversible process, so that retrograde metamorphic reactions do not affect the temperature estimates. This thermometer which is based on the quantification of the degree of ordering of CM with an intrinsic error calibration of 50 °C due to the petrological data used for calibration, but lower relative accuracy of about 15 °C (Beysac et al., 2004).

For temperature below 330 °C, Lahfid et al. (2010) performed a systematic study of the evolution of the Raman spectrum of CM in low-grade metamorphic rocks in the Glarus Alps (Switzerland). They showed that the Raman spectrum of CM is slightly different from the spectrum observed at higher temperature with additional peaks and they established a quantitative correlation between the degree of ordering of CM and temperature. We use this correlation, which is not a universal calibration (see discussion in Lahfid et al., 2010) to obtain first-order insights in the thermal evolution of rocks in the Casanova mélangé.

All Raman spectra were obtained using a Renishaw spectrometer following the analytical protocol described in Beyssac et al. (2002).

The results of our analysis (Table 2 and Fig. 8a,b) highlight the occurrence of two different temperature groups, the first one shows temperatures below c. 210°C, the second one shows temperature around 250°C. The first group includes all the samples from the matrix of the Casanova mélangé and from Helminthoid Flysch whereas the second is mainly formed of samples from the Internal Ligurian units but also of sliding blocks with similar lithology embedded within the Casanova mélangé.

The Taiwan mélanges: The Taiwan orogenic wedge (Fig. 9) is a newly (Plio-Quaternary) emerged active orogen allowing onland and offshore study of accretionary processes from oceanic subduction to continental subduction (e.g. Malavieille et al., 2002; Beyssac et al., 2007). South of the Taiwan Island, the oceanic lithosphere of the South China Sea (SCS) subducts beneath the Philippine Sea Plate (PSP), inducing since the early Miocene the development of the huge Manila accretionary wedge (e.g. Lewis and Hayes, 1984) and the volcanism of the Luzon arc (Ho, 1986). The northwestward motion of the PSP ($N306^\circ \pm 1^\circ$ azimuth), relative to the Eurasian plate (EP) has resulted in the progressive subduction of the thinned Chinese continental margin and the development of the Taiwan orogenic wedge (e.g. Suppe, 1984). North of $21^\circ 20'$ N, the wedge

becomes incorporated in the domain of continental margin subduction, involving progressively lower to middle Miocene slope and trench sediments (Reed et al., 1992). The southern tip of Taiwan Island represents the uplifted internal domain of the oceanic accretionary wedge currently undergoing the effects of the continental margin subduction (Lundberg et al., 1997; Reed et al., 1992; Huang et al., 1997; 2006; Chang et al., 2009). The retroside of the wedge extends offshore southward of the Hengchun Peninsula (HP) in the form of the Hengchun Ridge (HR) and Southern Longitudinal Trough (SLT) as far as 20°30'N (Malavieille et al., 2002; Lin et al., 2009; Lester et al., 2013). Different scenarios have been proposed for the tectonic evolution of the submarine accretionary wedge. In most models, the NW-SE oriented Kaoping Slope (KS) west of the subduction wedge of the Hengchun Ridge represents the part of the prism associated with the incipient subduction of the thinned Chinese continental margin (e.g. Huang et al., 1997; Liu et al., 1997; Malavieille et al., 2002; Chang et al., 2009; Malavieille & Trullenque, 2009; Mesalles et al., 2014). To the North, where the subduction of the southeastern margin of the Chinese continent is mature, the crust is now strongly deformed and rapidly uplifted in the Central Range of Taiwan (e.g., Simoes et al., 2007). This evolutionary setting (Fig. 10) has allowed the development of two different ophiolite bearing mélanges, the Kenting mélange which age range between 1 to 10 Ma and the 3.5~3.7 Ma old Lichi mélange whose formation processes are still debated. The detailed stratigraphic and structural characters and interpretations proposed for both mélange formations have been synthesized and discussed in Chang et al. (2009). The Kenting mélange is supposed to be a direct result of subduction processes acting in the forewedge. Following this hypothesis it is considered as a relict of the subduction channel developed at the base of the accretionary prism and then exhumed during collision (Chang et al., 2009). The Lichi mélange is regarded as a collision olistostromal mélange formed during forearc closure probably in relation with arcward backthrusting (e.g., Suppe and Liou, 1979 ; Page and Suppe, 1981 ; Huang et al., 2008), when the Luzon arc started to collide with the Eurasian continental margin following subduction of the oceanic lithosphere of the forearc area (Chang et al., 2009; Malavieille & Trullenque, 2009).

Input of analogue models on the interpretation of case studies

The differences in metamorphic history between Internal Ligurian units and External Ligurian ones (including the Casanova mélangé) revealed by RSCM thermometry are coherent with the results of previous studies based on illite and chlorite crystallinity (Molli et al., 1992; Marroni, 1994; Leoni et al., 1996; Ellero et al., 2001). Nevertheless, the new RSCM data enlight that the peak temperature is lower for the Casanova mélangé matrix than for the embedded blocks suggesting a different and deeper accretionary-related thermal history for the slided blocks elements embedded within the mélangé. It shows that a progressive exhumation of rocks from the deep parts of the wedge has occurred during basin development allowing the presence of metamorphic elements in the mélangé. These contrasted thermal histories are coherent with internal structures observed in cover-derived slided blocks (mainly stratal boudinage and isoclinal folding) similar to those of the Internal Ligurian Units (Pertusati and Horrenberger, 1975; Marroni and Pandolfi, 1996). Such structures are not observable within the Casanova mélangé matrix neither in the Helminthoid Flysch (Elter et al., 1991; Marroni et al., 1998; Marroni et al., 2002). The deeper - higher RSCM temperature – structural evolution of the Internal Ligurian units as well as those of the sedimentary cover-derived slide blocks within the Casanova mélangé are therefore developed in the Ligurian accretionary prism during the thickening stage.

All these observations can be interpreted in the light of experimental models, suggesting ophiolite accretion and burial in the wedge, exhumation through major backthrusting processes and gravity driven erosion in the retrowedge. Subsequent sedimentation on the upper-plate allows the formation of tectono-sedimentary ophiolite bearing mélanges in a forearc basin setting. The tectonic contact between Internal Ligurian units and the Casanova mélangé can be interpreted as a major backthrust of the Ligurian prism retroside (see for example the Exp. 3, Fig. 2c). In natural wedges, plastic deformation of sediments play an additional significant role favouring in some places overturning

of tectonic units by folding. The overturning of the Helminthoid Flysch unit including Casanova mélange (e.g., Marroni et al., 2002) as well as the internal tectonic-sedimentary features of the mélange itself could be related to deformation in the retrowedge. Although our simple models do not account for folding processes, they accurately describe exhumation and mélanges formation in a retrowedge setting. The kinematics of the main backthrust and associated large scale backfolding of basin units well account for the alpine deformation of the retroside of the Ligurian accretionary prism (Elter et al., 1991).

Results of our experiments allow refining former interpretations of the mechanisms responsible for Taiwan mélanges formation. The Figure 10 summarizes the geodynamic and tectonic setting for the two mélanges. The Kenting mélange that outcrops in the exhumed part of the accretionary wedge is most probably a remnant of ophiolite bearing tectonosedimentary mélanges previously formed in the subduction channel along the oceanic floor prowedge interface. Regarding our experiments (e.g., Exp.4, Fig. 3d) mélange units could be progressively incorporated in the forewedge thrust units during wedge growth, then passively backthrust, uplifted and incorporated in the retrowedge domain (Fig. 10a). During incipient subduction of the Eurasian continental margin, increasing shortening favors uplift and exhumation of the deep parts of the wedge allowing the Kenting mélange to reach the surface in the Hengchun Peninsula (Fig. 10b). Final exhumation occurred through denudation processes involving mass wasting in the retrowedge slope as illustrated in the experiments (see, Exp.4, Fig. 3d, Fig. 4b).

The Lichi mélange is related to the extreme shortening and backthrusting of the forearc basin that begins as a result of the subduction of a large piece of forearc basement (Malavieille & Trullenque, 2005, 2009). Mélange formation may result from two combined processes: (i) reworking of the backpart of the accretionary prism (including early ophiolitic mélanges) due to gravity driven submarine erosion and mass wasting in the forearc basin (Fig. 10a), and (ii) backthrusting of the forearc basin and subsequent incorporation of forearc basement ophiolitic debris along the eastern

tectonic contact of the basin (Fig. 10b). The Lichi mélange is then reworked during continental subduction and marks today the squeezed boundary between the strongly deformed volcanic arc (Coastal Range) and the Central Range of Taiwan orogenic wedge (Fig. 10c). As for the Casanova mélange, sampling of exotic blocks and matrix of the Lichi mélange was done for RSCM thermometry, unfortunately, the temperature was actually too low ($<210^{\circ}$) to be estimated by this method. More studies are needed to constrain the exhumation pathway of the materials of the mélange.

A genetic model for mélanges encountered in accretionary wedge settings

Based on insights from experiments and observations of natural examples of mélanges, we propose a genetic model for ophiolite bearing mélanges developed in accretionary wedge settings (Fig. 11). First, we consider that interactions between tectonics and submarine surface processes involving huge mass transfer of various materials during wedge evolution play a major role in mélange formation. During accretion, sediments mixed with ophiolitic fragments are underthrust and buried toward deep levels of the forewedge through the subduction channel. Part of it is accreted to the prism along seaward vergent imbricated thrusts (Fig. 11a). Simultaneously, major backthrusting and gravity driven erosion in the retrowedge allow exhumation of both deeply buried sediments from inside the wedge and offscraped (and sheared) ophiolitic debris (which have registered a peak of metamorphism during burial linked to the thickening of the accretionary prism). Primary mélanges developed in the subduction channel are exhumed thanks to retrowedge backthrusting, reworked by gravity driven surface processes and finally redeposited as tectono-sedimentary mélanges in the proximal basins located at the foot of the retrowedge slope. Temperature and pressure record of exhumed blocks deposited in the forearc basin mélanges reflect the history and evolution of wedge thickening through time (Fig. 11a). In the basin, mélange deposits are continuously involved in backthrusting induced synsedimentary shear deformation (e.g., Alonso et

al., 2015). Simultaneously, widespread overturning of retrowedge basin sequences can occur due to large scale folding processes. An additional tectonic process can favour the incorporation of ophiolitic material and subsequent exhumation in the retrowedge (Fig. 11b). If a décollement exists in the trench fill sediments, it will allow basal accretion and underplating at depth of sedimentary materials mixed with ophiolitic debris. Then, gravity driven erosional processes combined with backthrusting exhume these rocks allowing déposition of mélange formations in the retrowedge basin.

Acknowledgements: This work has benefited of funding in the frame of the French Syster INSU Project and of the LIA D3E, C.N.R.S.-M.O.S.T. France-Taiwan International Laboratory.

C. Romano is warmly acknowledged for his crucial technical help during the experimental work.

Figures caption

Figure 1: a) Experimental set-up. b) Cartoon illustrating the main characters of a doubly vergent sandwedge submitted to asymmetrical shortening. The slope angle, a possible geometry and behaviour of the prowedge and retrowedge is suggested. S represents the velocity discontinuity.

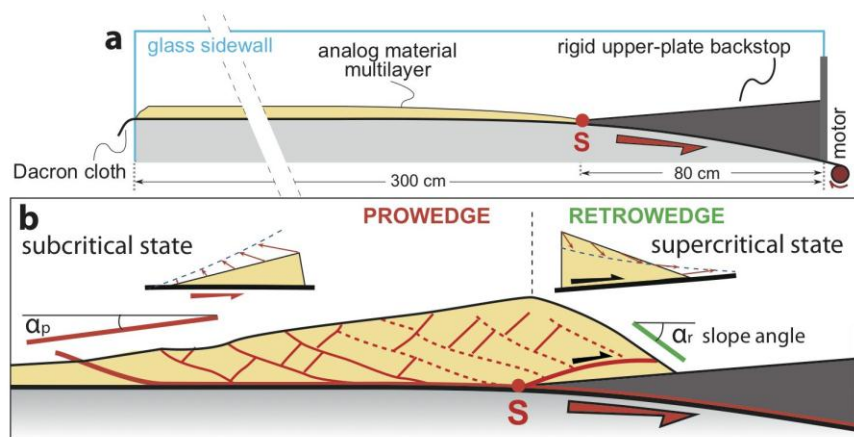


Figure 1

Figure 2: A) Setting of described experiments and composition of models before shortening. Model ophiolite-bearing sediments are in green. B) Pictures of each experiment at the end of shortening deformation.

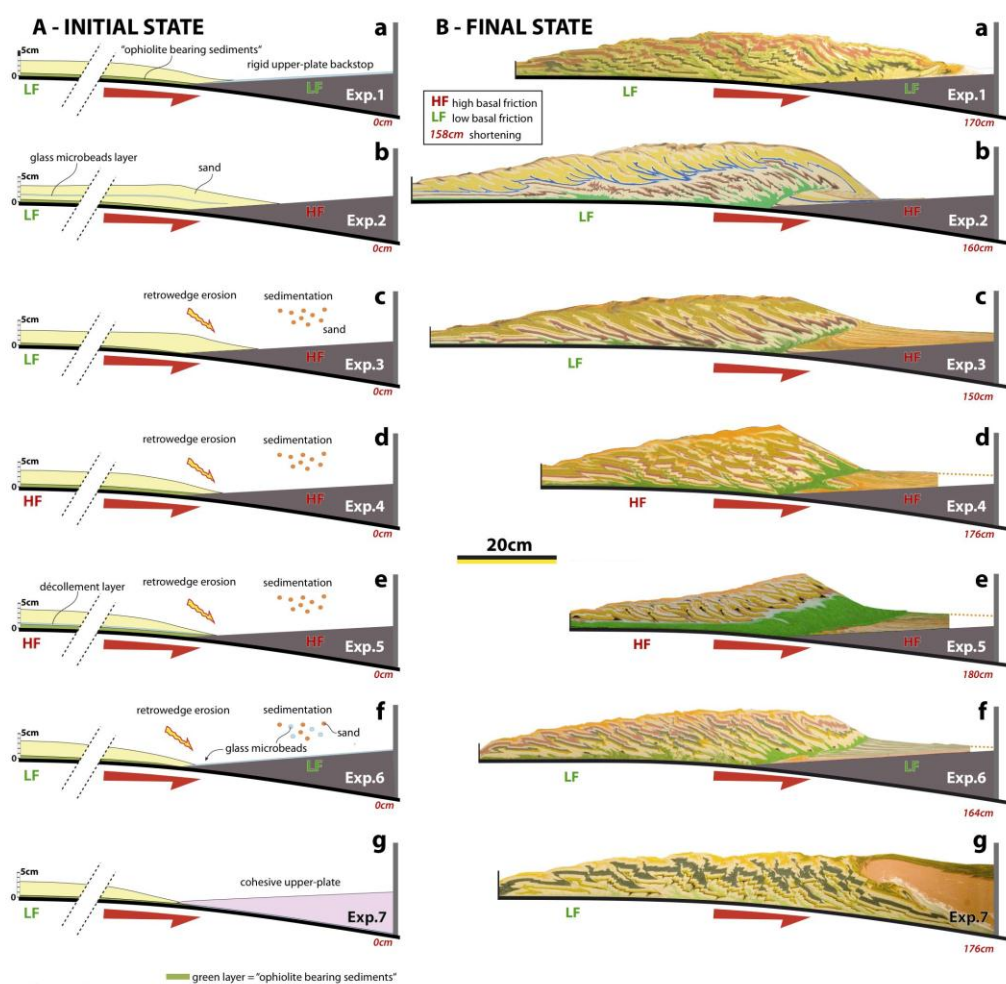


Figure 2

Figure 3: Schematic drawing of the final stages of experiments at the same scale. Experiments 1, 2 and 7 are run without erosion. Experiments 3, 4, 5 and 6 involve erosion and sedimentation on the upper-plate backstop. A detailed description of each experiment is given in the text.

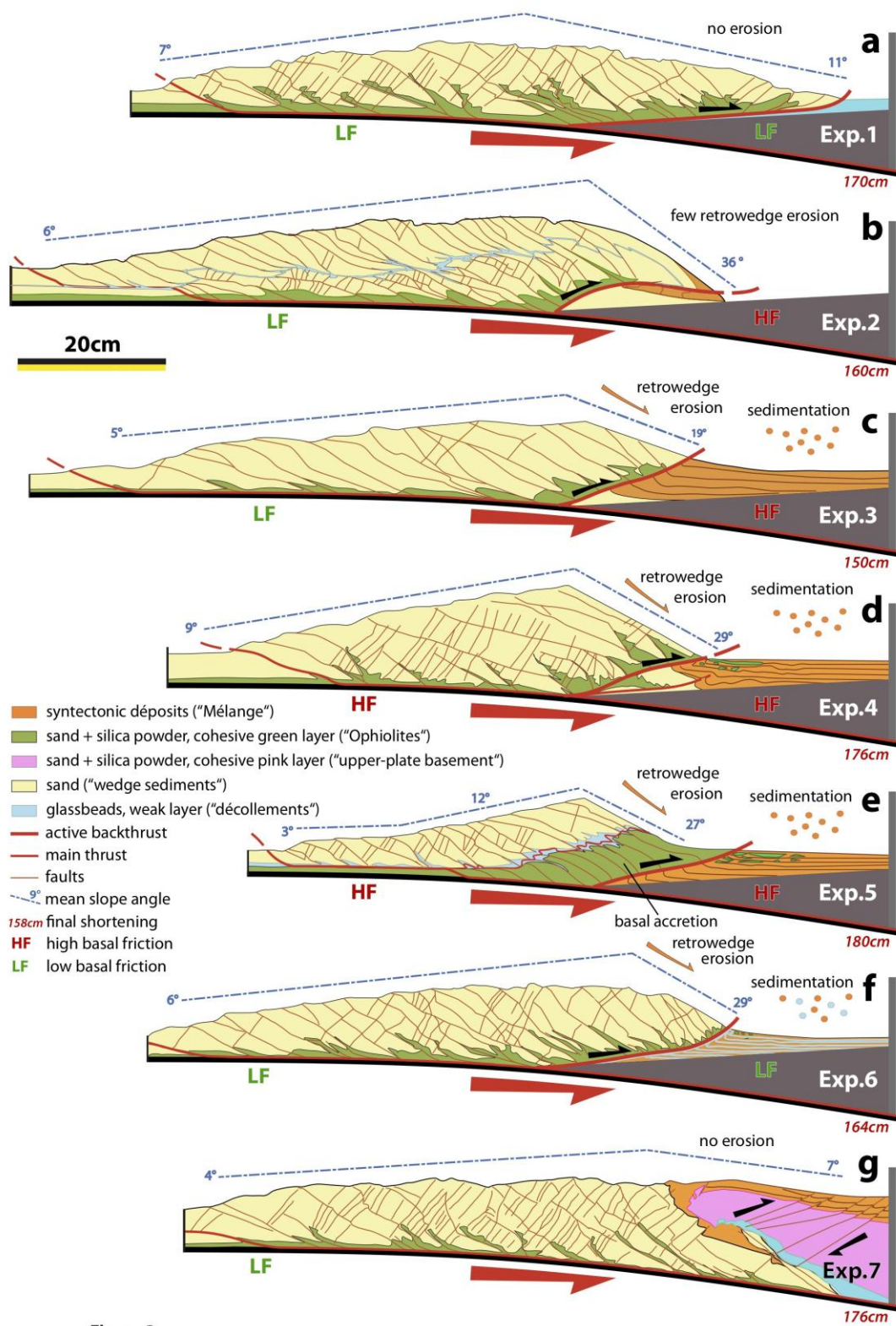


Figure 3

Figure 4: Evolutionary stages of experiments 3 and 4 outlining the impact of basal friction on wedge dynamics and exhumation.

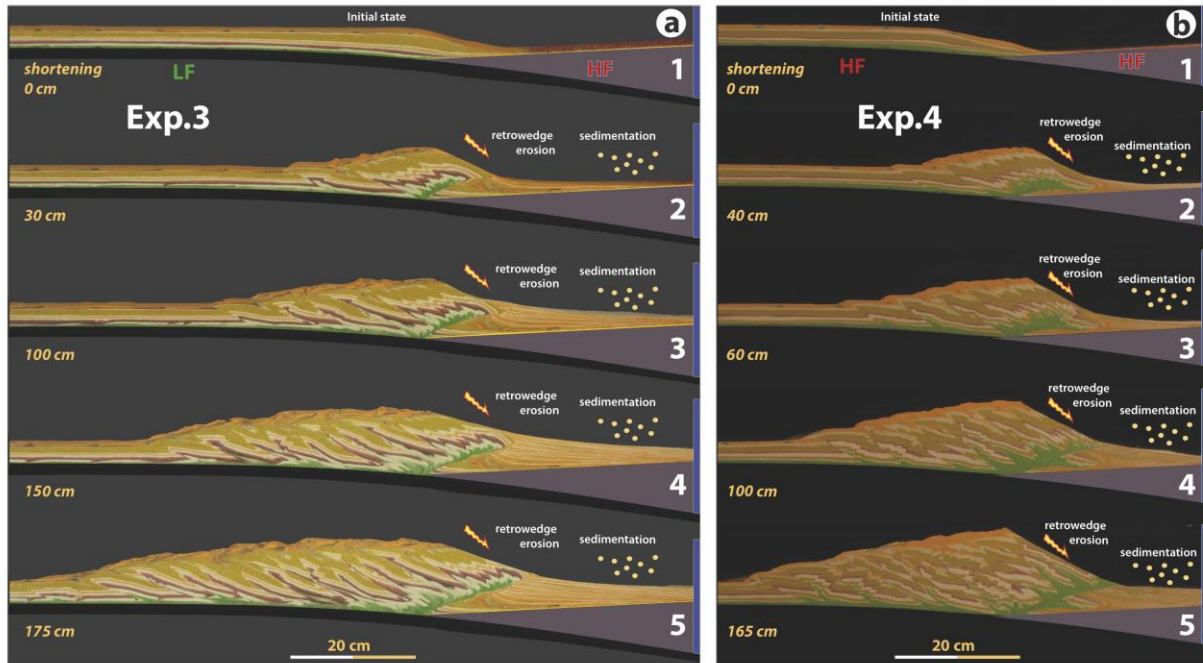


Figure 4

Figure 5: Oblique view of experiment 5 showing basal accretion, exhumation of the green layer (model ophiolites) in the retrowedge and “mélange” formation in the basin.

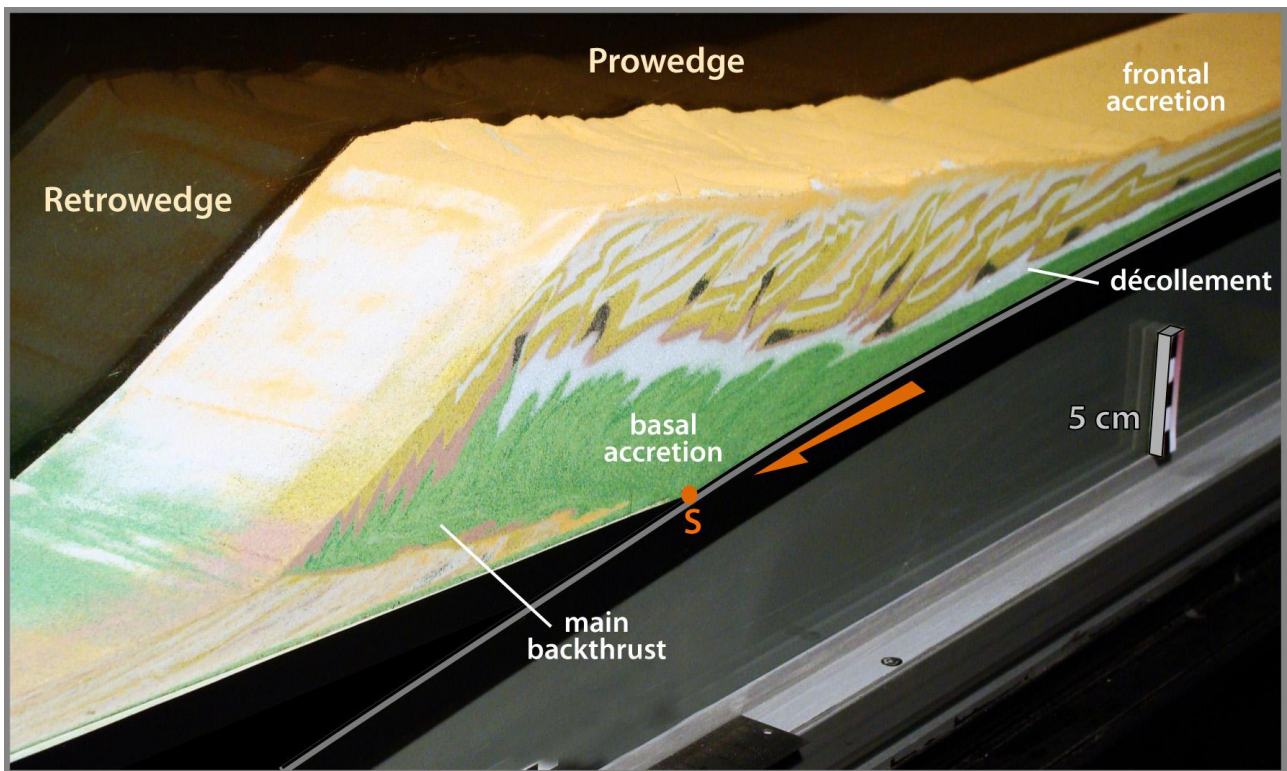


Figure 6: Example of quantitative analysis applied to all experiments. Consecutive high quality images are processed using image correlation techniques. Comparison between two steps allows to determine the displacement field, the amplitude of movements, the amplitude of vertical and horizontal components of displacement (a, b, c, d) and to reconstruct the paths followed by particles of material during shortening (e).

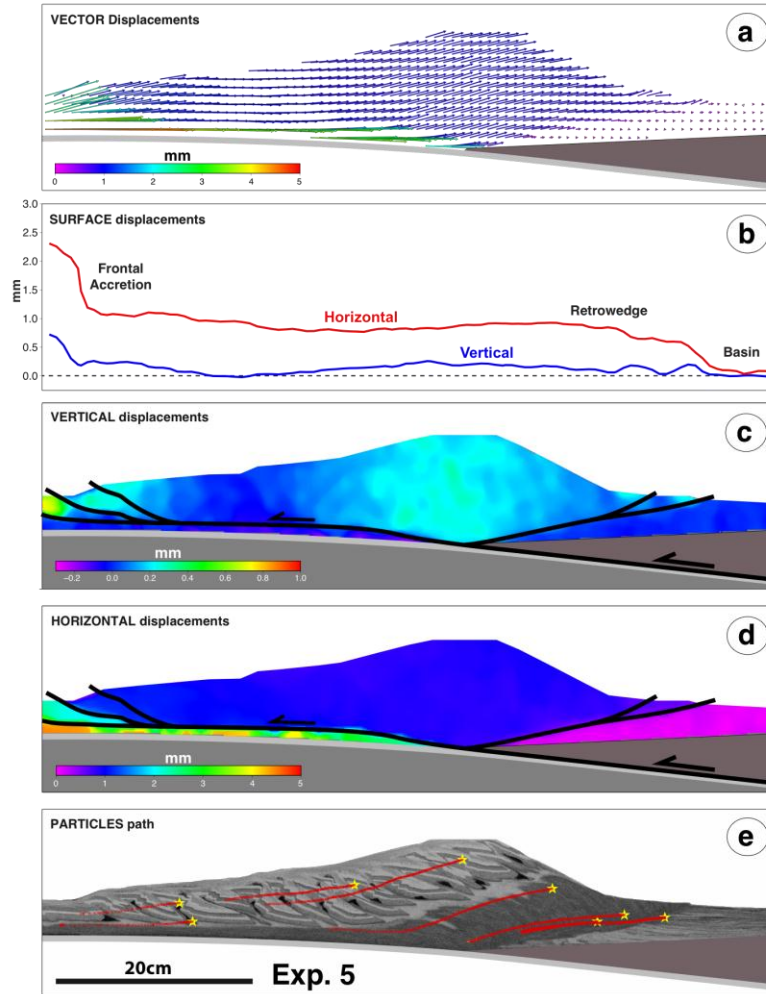


Figure 6

Figure 7: Setting of the Casanova mélangé: a) In the general frame of the alpine arc.

b) At the scale of the regional geological map. The main tectonic units are outlined. For the Western Alps: (1,2) Europe-derived external Alpine units. 1) Alpine foreland units; (2) External massifs (Ar, Argentera and P, Pelvoux); (3) Middle Penninic Briançonnais nappes (4) Middle Penninic Internal Massif (DM, Dora Maira and GP, Gran Paradiso); (5) Upper Penninic Helminthoid Flysch: UE, Ubaye-Embrunais, Western Liguria Helminthoid Flysch (WL) and the Antola unit (A). With the same color are also represented the ophiolitic non-metamorphic unit of Chenaillet (Ch) and Sestri Voltaggio Zone (SVZ) and the Antola nappe (A) (6) Schistes Lustrés composite nappe system; (7) Sesia and related units (“lower Austroalpine nappes”); (8) Adria lower crust of the Southern Alps (Ivrea); (9) Adria upper crust basement and cover of the Southern Alps; Northern Apennine: (10) Internal Ligurian units, IL; (11) External Ligurian units (EL) and SubLigurian (Canetolo) units; (12, 13, 14) Adria-derived Tuscan and external foreland Umbria-Marche units; (12) Cervarola and Umbria-Marche foreland units (13) Tuscan nappe; (14) Tuscan metamorphic units; ; (15) Post-tectonic cover of Tertiary Piemontese basin and Epiligurian units; (16) Neogene and Quaternary sediments of Po Plain and inner Tuscany. Bo: Bobbio tectonic window (see cross-section); ALB alpine Ligurian backthrust.

c) Schematic cross section of the northern Apennines chain close to Casanova area (modified from Molli, 2008).

d) The alpine accretionary wedge at the end of Cretaceous. Schematic map and section.

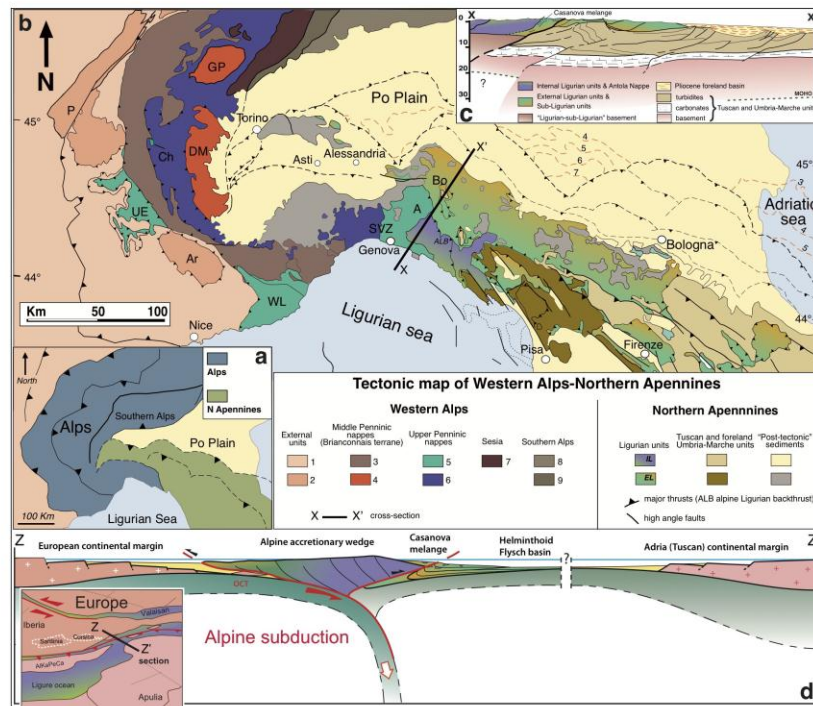


Figure 7

Figure 8: a) Detailed geological map of the Casanova mélange and b) cross section (modified from Elter et al., 1991). Results of the thermometry analysis are reported (coloured dots and related temperatures).

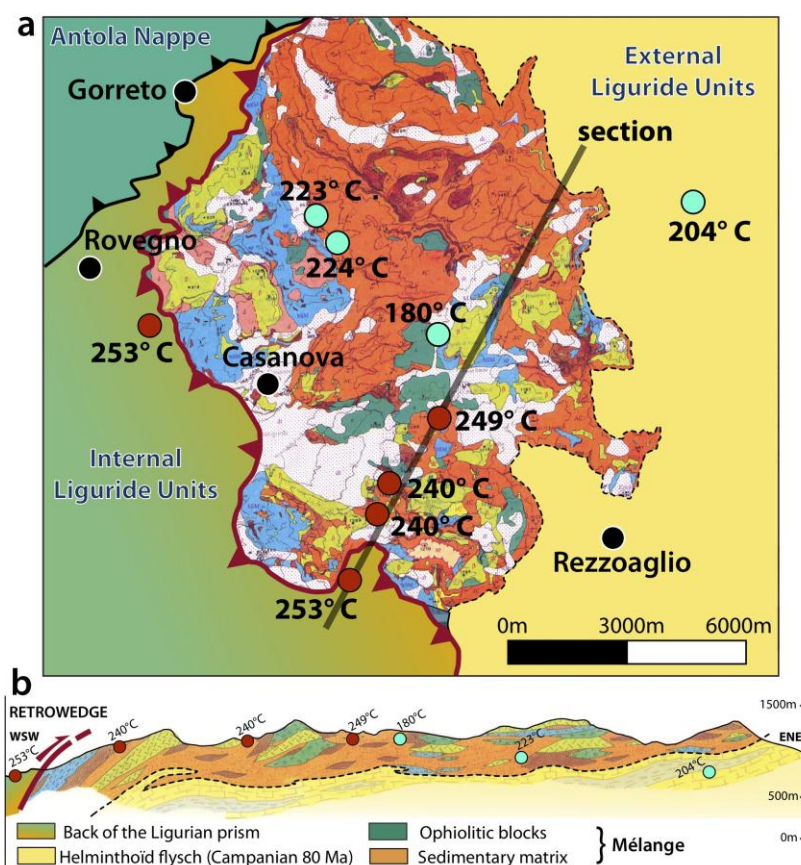


Figure 8

Figure 9: Structural sketch map of Taiwan showing the setting of the Kenting and Lichi mélanges (green stars) in the frame of the orogenic wedge. Caption: - Eurasian Plate: 1 Asian continental margin & foreland basin, 2 Oceanic crust of the south China Sea, 3 Western Foothills and Kaoping Slope (Miocene-Pleistocene series of the syn-collision orogenic wedge), 4 Pre-collision oceanic accretionary wedge, 5 Underthrust Paleogene sequences of the Eurasian continental margin, 6 Extended continental crust (Okinawa back-arc basin), 7 Uplifted core of the pre-collision oceanic accretionary wedge, 8 Eocene series of the Eurasian continental margin, 9 Pre-tertiary metamorphic rocks of the Eurasian continental margin, 10 Exhumed HP rocks of the Yuli belt, 11 Pleistocene-Holocene sediments of the Southern Longitudinal Trough and Longitudinal Valley orogenic basins. - Philippine Sea Plate: 12 forearc basins and deformed forearc sediments of the Huatung Ridge, 13 Accreted volcanic edifices and forearc sediments of the Luzon arc, 14 Luzon volcanic arc, 15 Oceanic crust of the Philippine Sea Plate, 16 Ryukyu accretionary wedge, M mélanges outcrops.

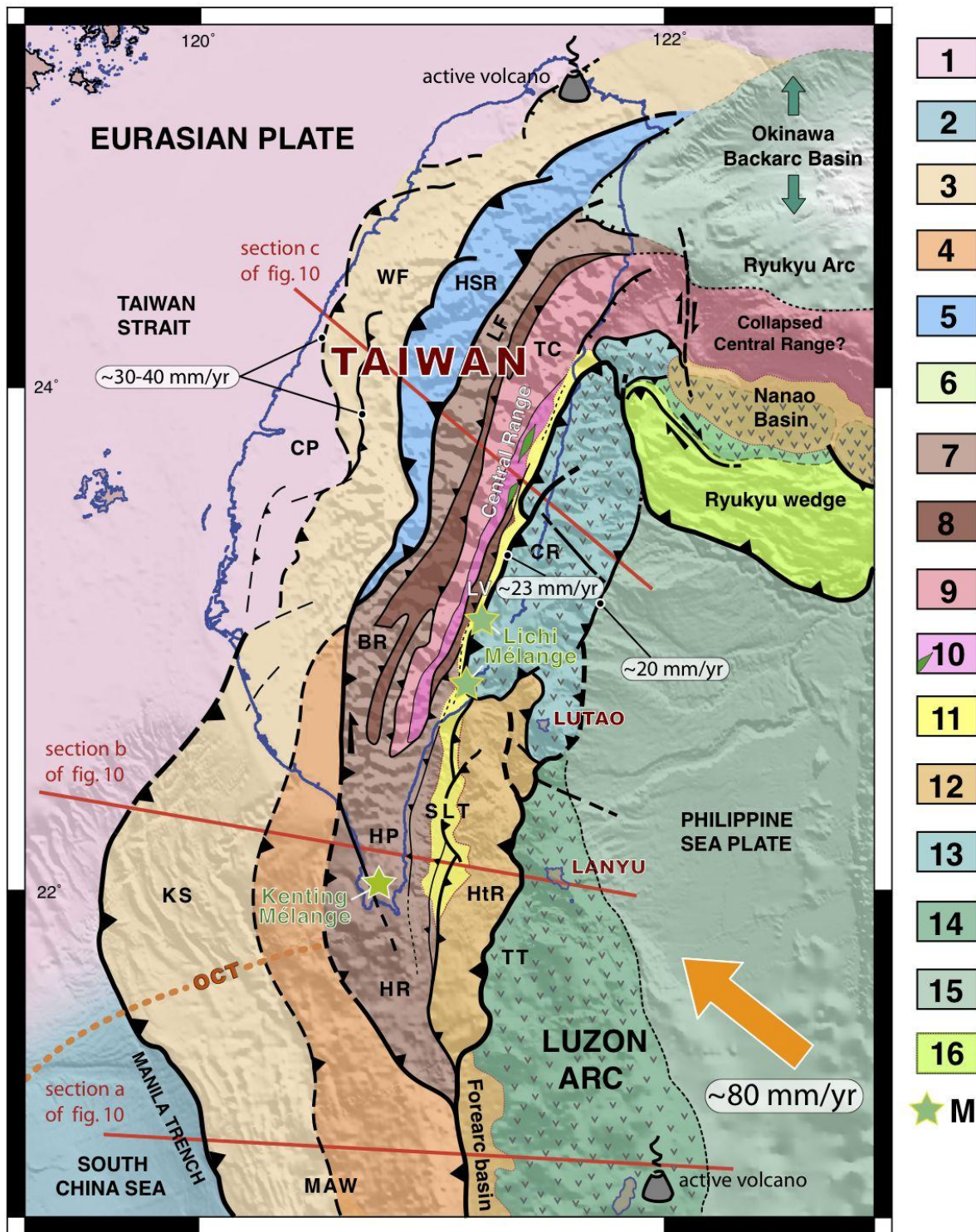


Figure 9

Figure 10: Interpretative E-W cross-sections (see location on figure 9) showing the general geodynamic situation and evolution of the Taiwan orogen from south to north, from oceanic to continental subduction. a) Oceanic subduction stage with development of the sedimentary accretionary wedge. b) Stage showing the incipient subduction of the extended Eurasian continental margin. c) Subduction of the Continental margin and development of the Taiwan orogenic wedge. At each stage, the zooms outline the main tectonic processes inferred from experimental results for the accretion of ophiolites in the prism and subsequent formation of tectonosedimentary mélanges .

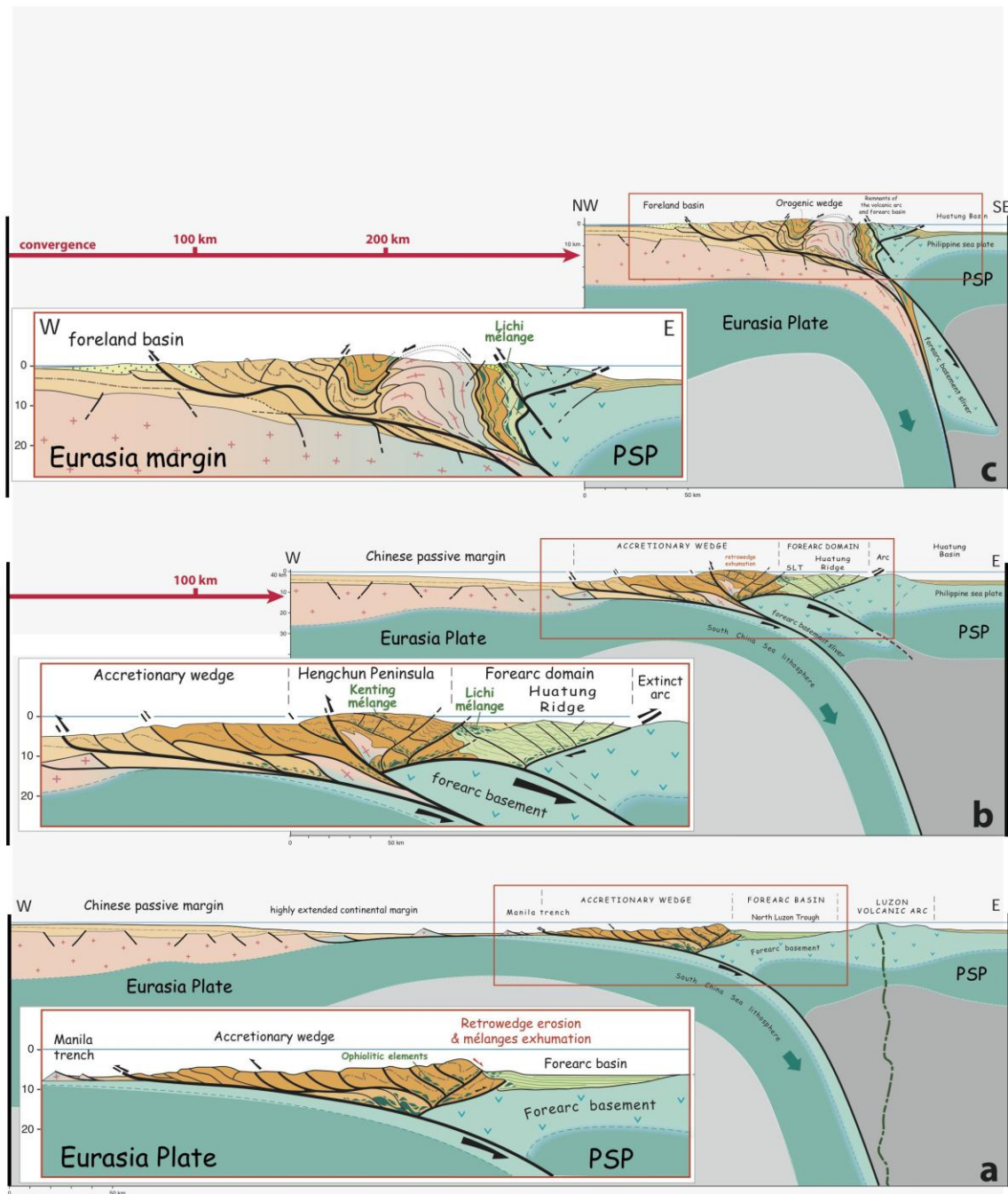


Figure 10

Figure 11: Cartoon illustrating the proposed model for exhumation and redeposition of ophiolitic debris and wedge rocks as tectonosedimentary mélanges in the retrowedge setting. Major backthrusting and gravity driven submarine erosion allows exhumation and deposition of exotic blocks in the syn-tectonic retrowedge basin. a) First setting, the wedge grows by frontal accretion of imbricated thrust units. The red dotted lines suggest the shape of isotherms registered by peak temperature thermometry. b) Second setting, deformation partitioning occurs, the wedge grows by frontal accretion and basal accretion at depth.

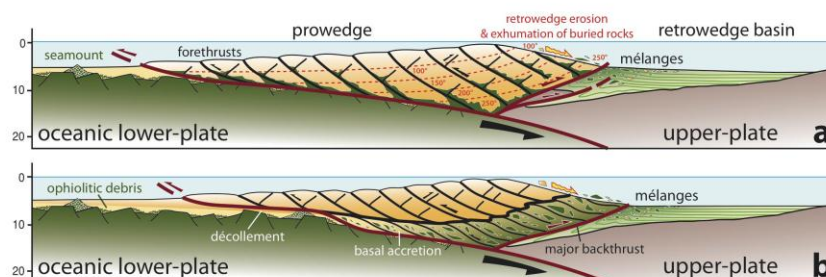


Figure 11

Table 1: Characteristics of the analog materials used in experiments.

| Analog material | Aeolian sand | Glass microbeads | Silica powder |
|------------------------------|--------------|------------------|---------------|
| Density (Kg/m ³) | 1690 | 1700 | 1900 |
| Internal friction | 0,57 | 0,44 | 1,00 |
| Size (µm) | 300 | 100 to 200 | 43 |
| Cohesion (Pa) | 20 | negligible | 150 |

Table 2: Sample location and results of thermometry analysis in the Casanova mélange.

| Sample | X | Y | T °C |
|--------|-------------|-------------|-------|
| 1 | 9,328813388 | 44,52303951 | 252,5 |
| 4 | 9,335029893 | 44,53367575 | 240 |
| 6 | 9,337756614 | 44,53866208 | 240 |
| 7 | 9,349092057 | 44,54916818 | 248,7 |
| 10 | 9,348834793 | 44,56265869 | cold |
| 14 | 9,263170850 | 44,61577554 | 230 |
| 15 | 9,326047905 | 44,57743818 | 224,5 |
| 16 | 9,321242787 | 44,58192393 | 223 |
| 19 | 9,283515029 | 44,56408829 | 253 |
| 26 | 9,406562579 | 44,58400344 | 204 |
| 28 | 9,501482188 | 44,53604419 | 209 |
| 29 | 9,333451924 | 44,50793759 | 245,6 |
| 30 | 9,209893517 | 44,51319619 | 251 |

Additional material:

Movie 1: Movie of the experiment 1 run without erosion.

Movie 2: Movie of the experiment 3 run with retrowedge erosion and sedimentation. Notice the exhumation of the green layer.

References

- Alonso, J.L., Marcos, A., and Suárez, A., 2006, Structure and organization of the Porma mélange: Progressive denudation of a submarine nappe toe by gravitational collapse: *American Journal of Science*, v. 306, p. 32–65. doi:10.2475/ajs.306.1.32
- Alonso, J.L., Marcos, A., Villa, E., Suárez, A., Merino-Tomé, O. A., and Fernández, L.P., 2015,

Mélanges and other types of block-in-matrix formations in the Cantabrian Zone (Variscan Orogen, northwest Spain): origin and significance: *International Geology Review*, v. 57, p. 563–580.

doi:10.1080/00206814.2014.950608.

Argnani, A., Fontana, D., Stefani, C., Zuffa, G.C., 2004. Late Cretaceous Carbonate Turbidites of the Northern Apennines: Shaking Adria at the Onset of Alpine Collision *Journal of Geology*, 112, 251–259 d.o.i. 0022-1376/2004/11202-0007

Barber, T., and Brown, K., 1988. Mud diapirism: the origin of melanges in accretionary complexes ? *Geology Today*, 4, pp. 89–94

Beaumont, C., and Pfiffner, A., 1999. Dynamics of sediment subduction-accretion at convergent margins : Short-term modes, long-term deformation, and tectonic implications. *Journal of Geophysical Research*, 104, 17573-17601.

Bennett, R.A., Serpelloni, E., Hreinsdottir, S., Brandon, M.T., Buble, G., Basic, T., Casale, G., Cavaliere, A., Anzidei, M., Marjonovic, M., Minelli, G., Molli, G., Montanari, A. et al., 2012. Syn-convergent extension observed using the RETREAT GPS network, northern Apennines, Italy. *Journal of Geophysical Research*, 117, B04408.

Beysac, O., Goffé, B., Chopin, C., & Rouzaud, J.-N., 2002. Raman spectra of carbonaceous material in metasediments : a new geothermometer. *Journal of Metamorphic Geology* , 20, 859-871.

Beysac, O., Bollinger, L., Avouac, J.P., & Goffe, B., 2004. Thermal metamorphism in the lesser Himalaya of Nepal determined from Raman spectroscopy of carbonaceous material. *Earth and Planetary Science Letters*, 225, 233-241.

Beysac, O., Simoes, M., Avouac, J.P., Farley, K.A., Chen, Y.G., Chan, Y.C., Goffé, B., 2006. Late Cenozoic metamorphic evolution and exhumation of Taiwan. *Tectonics* 26, TC6001. doi:10.1029/2006TC002064.

Bettelli, G., and Vannucchi, P., 2003. Structural Styles of offscrapped Ligurian oceanic sequences of the Northern Apennines: new hypothesis concerning the development of mélangé block-in-matrix fabric. *Journal of Structural Geology*, 25, 371-388.

Bonnet, C., 2007. Interactions between tectonics and surface processes in Alpine foreland : Insights from analog model and analysis of recent faulting. Ph. D. thesis, Université Montpellier 2.

Bettelli, G., and Panini, F., 1989, I mélanges dell'Appennino settentrionale tra il T. Tresinaro ed il T. Sillaro: *Memorie Della Società Geologica Italiana*, v. 39, p. 187–214.

Boccaletti, M., Elter, P., Guazzone, G., 1971, Plate tectonic models for the development of the Western Alps and Northern Apennines. *Nature* 234:108–111.

Bonini, M., 2006, Detachment folding–related Miocene submarine slope instability in the Romagna Apennines (Italy), *J. Geophys. Res.*, 111, B01404, doi:10.1029/2004JB003552.

Brandon, M.T., 1989, Deformational styles in a sequence of olistostromal mélanges, Pacific Rim Complex, western Vancouver Island, Canada: *Geological Society of America Bulletin*, v. 101, p. 1520–1542.

Carminati, E., and Doglioni, C., 2012. Alps vs. Apennines: The paradigm of a tectonically

asymmetric Earth. *Earth Sciences Reviews*, 112 (2012) 67–96.

Cerrina Feroni A, Leoni L, Martelli L, Martinelli P, Ottria G, Sarti G. 2001. The Romagna Apennines, Italy: an eroded duplex. *Geological Journal* 36: 39–54.

Cerrina Feroni, A., Ottria, G., Martinelli, P., Martelli, L., 2002. Structural Geological Map of the Emilia-Romagna Apennines. Regione Emilia-Romagna and CNR, SELCA Firenze.

Chang, P-C., Angelier, J. and Huang, C-Y., 2009. Evolution of Subductions Indicated by Mélanges in Taiwan. S. Lallemand and F. Funiciello (eds.), *Subduction Zone Geodynamics*, 207, DOI 10.1007/978-3-540-87974-9,

Cloos, M., 1984. Flow melanges and the structural evolution of accretionary wedges, in: L.A. Raymon (Ed.), *Mélanges: Their Nature, Origin and Significance*, Special Paper-Geological Society of America, 198 (1984), pp. 71–79

Cloos, M., and Shreve, R.L., 1988, Subduction channel model of prism accretion, mélange formation, sediment subduction, and subduction erosion at convergent plate margins: 2. Implications and description: *Pure and Applied Geophysics*, v. 128, p. 501–545, doi: 10.1007/BF00874549 .

Codegone, G., Festa, A., Dilek, Y., and Pini, G.A., 2012, Smallscale polygenetic mélanges in the Ligurian accretionary complex, Northern Apennines, Italy, and the role of shale diapirism in superposed mélange evolution in orogenic belts: *Tectonophysics*, v. 568-569, p. 170–184. doi:10.1016/j. tecto.2012.02.003

Cowan, D.S., 1985, Structural styles in Mesozoic and Cenozoic mélanges in the western Cordillera of North America: Geological Society of America Bulletin, v. 96, p. 451–462.

Dahlen, F., 1984. Non cohesive critical coulomb wedges; an exact solution. Journal of Geophysical Research, 89, 10125-10133.

Dahlen, F.A., Suppe, J., Davis, D., 1984. Mechanics of fold-and-thrust belts and accretionary wedges: cohesive coulomb theory. Journal of Geophysical Research 89 (B12), 10087–10101.

Daniele, G., and Plesi, G., 2000. The Ligurian Helminthoid flysch units of the Emilian Apennines: stratigraphic and petrographic features, paleogeographic restoration and structural evolution. Geodinamica Acta 13: 1–21.

Davis, D., Suppe, J., Dahlen, F.A., 1983. Mechanics of fold-and-thrust belts and accretionary wedges. Journal of Geophysical Research 88 (B12), 1153–1172.

Davy, P., Cobbold, P.R., 1991. Experiments on shortening of a 4-layer model of the continental lithosphere. Tectonophysics 188 (1–2), 1–25.

Del Castello, M., Mc Clay, K. R., Pini, G.A., 2005. Role of pre-existing topography and overburden on strain partitioning of oblique doubly vergent convergent wedges. Tectonics, 24, TC6004, doi:10.1029/2005TC001816.

Doglioni, C., Mongelli, F., Pialli, G., 1998. Boudinage of the Alpine belt in the Apenninic back-arc. Memorie della Societa Geologica Italiana 52:457–468.

Dominguez, S., Lallemand, S.E., Malavieille, J. and Von Huene, R., 1998. Upper plate deformation associated with seamount subduction, *Tectonophysics*, 293, 207-224.

Dominguez, S., Lallemand, S., Malavieille, J. and Schnurle, P., 1998. Oblique subduction of the Gagua Ridge beneath the Ryukyu accretionary wedge system: Insights from marine observations and sandbox experiments. *Marine Geophysical Researches*, Vol. 20, 383-402.

Dominguez, S., Malavieille, J., and Lallemand, S.E., 2000. Deformation of margins in response to seamount subduction: Insights from sandbox experiments, *Tectonics*, Vol. 19, (1), 182-196.

Ellero, A., Leoni, L., Marroni, M., and Sartori, F., 2001. "Internal Liguride units from central Liguria, Italy; new constraints to the tectonic setting from white mica and chlorite studies. *Schweizerische Mineralogische Und Petrographische Mitteilungen, Bulletin Suisse De Mineralogie et Petrographie*, 81, no. 1: 39-53.

Elter, P., (1975) Introduction à la géologie de l'Apennin septentrional. *Bulletin de la Société Géologique de France* 7: 956-96.

Elter, P., Marroni, M., Molli, G., Pandolfi, L., (1991). Le caratteristiche stratigrafiche del complessodi M.Penna/Casanova, Alta Val di Trebbia, Appennino settentrionale. *Atti Ticinensi di Scienze della Terra*, 34, 97-106.

Elter, P., 1997. Detritismo ofiolitico e subduzione: riflessioni sui rapporti Alpi e Appennino. *Memorie della Societa` Geologica Italiana* 49:205-215

Festa, A., Pini, G-A., Dilek, Y., Codegone, G., 2010. Mélanges and mélange-forming processes: a

historical overview and new concepts, *International Geology Review*, Vol. 52, (10–12), 1040–1105.

Festa, A., Ogata, K., Pini, G-A., Dilek, Y., Codegone, G., 2014. Late Oligocene–early Miocene olistostromes (sedimentary mélanges) as tectono-stratigraphic constraints to the geodynamic evolution of the exhumed Ligurian accretionary complex (Northern Apennines, NW Italy), *International Geology Review*, DOI:10.1080/00206814.2014.931260

Ghikas, A.C., Dilek, Y., and Rassios, A.E., 2010, Structure and tectonics of sub-ophiolitic mélanges in the Western Hellenides (Greece) and implications for Ophiolite emplacement tectonics: *International Geology Review*, v. 52, p. 423–453.

Graveleau, F., Hurtrez, J.-E., Dominguez, S., Malavieille, J., 2011. A new experimental material for modeling interactions between tectonics and surface processes. *Tectonophysics* 513 (1–4), 68–87.

Graveleau, F., Malavieille, J., Dominguez, S., 2012. Experimental modelling of orogenic wedges: A review, *Tectonophysics*, Volumes 538–540, 4 May 2012, Pages 1–66. doi: 10.1016/j.tecto.2012.01.027.

Gutscher, M-A., Kukowski, N., Malavieille, J., Lallemand, S., 1996. Cyclical behavior of thrust wedges : Insights from high basal friction sandbox experiments. *Geology*, 24, 135-138.

Gutscher, M-A., Kukowski, N., Malavieille, J., Lallemand, S., 1998a. Material transfer in accretionary wedges from analysis of systematic series of analog experiments. *Journal of Structural Geology*., 20, 407-416.

Gutscher, M.A., Kukowski, N., Malavieille, J., and Lallemand, S., 1998b, Episodic Imbricate

thrusting & underthrusting; Analog experiments and Mechanical Analysis applied to the Alaskan Accretionary Wedge. *J. Geophys. Res.*, 103, 10,161-10,176.

Hajna, J., Zac, J., and Kachlik, V., 2014. Growth of accretionary wedges and pulsed ophiolitic mélangé formation by successive subduction of trench-parallel volcanic elevations. *Terra Nova*, Vol 26, No. 4, 322–329

Hampton, M.A., Lee, H.J., and Locat, J., 1996, Submarine landslides: Reviews of Geophysics, v. 34, p. 33–59. doi:10.1029/95RG03287

Harders, R., Ranero, C.R., Weinrebe, W., and Behrmann, J.H., 2011, Submarine slope failures along the convergent continental margin of the Middle America Trench: Geochemistry: Geophysics, Geosystems, v. 12, p. Q05S32.

Hernaiz Huerta, P. P.; Pérez-Valera, F.; Abad, M.; Monthel, J.; Diaz de Neira, A. 2012. Melanges and olistostromes in the Puerto Plata area (northern Dominican Republic) as a record of subduction and collisional processes between the Caribbean and North-American plates. *Tectonophysics*, Elsevier, 568, pp.266-281. DOI :10.1016/j.tecto.2011.10.020

Hooke, R.L., 2003. Time constant for equilibration of erosion with tectonic uplift. *Geology*, 31, 7, 621-624.

Horsfield, W., 1977. An experimental approach to basement-controlled faulting. *Geologie en Mijnbouw* 56 (4), 363–370.

Hoth, S., Adam, J., Kukowski, N., and Oncken, O., 2006. Influence of erosion on the kinematics of

bivergent orogens. Results from scaled sandbox simulations. In: Willett, S.D., Hovius, N., Brandon, M.T. & Fisher, D.M. (eds) *Tectonics, Climate, and Landscape Evolution*. Geological Society of America, Special Papers, 398, 201–225.

Hoth, S., Homann-Rothe, A., and Kukowski, N., 2007. Frontal accretion: An internal clock for bivergent wedge deformation and surface uplift. *Journal of Geophysical Research*, 112, B6, B06408. DOI: <http://doi.org/10.1029/2006JB004357>.

Hsu, T., 1956. Geology of the Coastal Range, eastern Taiwan. *Bull Geol Surv Taiwan*, 8, 39-63.

Hsü, K.J., 1965, Franciscan rocks of Santa Lucia Range, California, and the ‘argille scagliose’ of the Appennines, Italy: A comparison in style of deformation: *Geological Society of America Abstracts for 1965*, p. 210–211.

Hsü, K.J., 1968. Principles of mélanges and their bearing on the Franciscan-Knoxville Paradox: *Geological Society of America Bulletin*, v. 79, p. 1063–1074.

Huang, C.-Y., Wu, W.-Y., Chang, C.P., Tsao, S., Yuan, P.B., Lin, C.W., Kuan-Yuan, X., 1997. Tectonic evolution of accretionary prism in the arc-continent collision terrane of Taiwan. *Tectonophysics* 281, 31–51.

Huang, C-Y., Yuan, P-B., Tsao, S-J., 2006. Temporal and spatial records of active arc-continent collision in Taiwan : a synthesis. *GSA Bulletin*; March/April 2006; v. 118; no. 3/4; p. 274–288; doi: 10.1130/B25527.1.

Huang, C.Y., Chien, C.W., Yao, B., and Chang, C.P., 2008, The Lichi mélange: A collisional

mélange formation along early arcward backthrusts during forearc basin closure, Taiwan arc-continent collision, in Draut, A.E., Clift, P.Do., and Scholl, D.W., eds., Formation and applications of the sedimentary record in arc collision zones: Geological Society of America Special Paper 436, p. 127–154.

Hubbert, M.K., 1937. Theory of scale models as applied to the study of geologic structures. *Bulletin of the Geological Society of America* 48 (10), 1459–1519.

Hubbert, M.K., 1951. Mechanical basis for certain familiar geologic structures. *Bulletin of the Geological Society of America* 62 (4), 355–372.

Jeanbourquin, P., Kindler, P., and Dall’Agnolo, S., 1992, Les mélanges des Préalpes internes entre Arve et Rhône (Alpes occidentales franco-suissees): *Eclogae Geologicae Helvetiae*, v. 85, p. 59–83.

Jolivet, L., Faccenna, C., Goffé, B., Mattei, M., Rossetti, F., Brunet, C., Storti, F., Funicello, C., Cadet, J.P., D’Agostino, N., Parra, T., 1998. Midcrustal shear zones in postorogenic extension: example from the northern Tyrrhenian Sea. *J Geophys Res* 103:12123–12160

Kimura, G., and Mukai, A., 1991, Underplated units in an accretionary complex: Mélangé of the Shimanto belt of eastern Shikoku, southwest Japan: *Tectonics*, v. 10, no. 1, p. 31–50.

Konstantinovskaya, E., and Malavieille, J., 2005. Erosion and exhumation in accretionary orogens : Experimental and geological approaches. *Geochemistry, Geophysics, Geosystems*, Vol. 6, (2), 25pp, Q02006, doi:10.1029/2004GC000794, ISSN: 1525-2027

Konstantinovskaya, E., and Malavieille, J., 2011. Thrust wedges with decollement levels and

syntectonic erosion : a view from analog models. *Tectonophysics*, 502, 336-350.

Krantz, R.W., 1991. Measurements of friction coefficients and cohesion for faulting and fault reactivation in laboratory models using sand and sand mixtures. *Tectonophysics* 188 (1–2), 203–207.

Kukowski, N., Lallemand, S., Malavieille, J., Gutscher, M.-A., and Reston, T., 2002. Mechanical decoupling and basal duplex formation observed in sandbox experiments with application to the western mediterranean ridge accretionary complex. *Marine Geology*, 186, 29-42.

Labauve, P., 1992, Evolution tectonique et sédimentaire des fronts de chaîne sous-marins. Exemples des Apennins du Nord, des Alpes française ed de Sicilie [Thèse de Docteur D'Etat]: Montpellier, Universitie Montpellier II, 476 p.

Lahfid, A., Beyssac, O., Deville, E., Negro, F., Chopin, C., and Goffé, B., 2010. Evolution of the Raman spectrum of carbonaceous material in low-grade metasediments of the Glarus Alps (Switzerland). *Terra Nova*, Vol 22, No. 5, 354. doi: 10.1111/j.1365-3121.2010.00956.x

Lallemand, S. E., Malavieille, J., and Calassou, S., 1992. Effects of oceanic Ridge subduction on accretionary wedges: Experimental modeling and marine observation., *Tectonics*, 11, 1301-1313.

Lallemand, S.E., Schnurle. P., & Malavieille, J., 1994. Coulomb theory applied to accretionary and non-accretionary wedges - possible causes for tectonic erosion and/or frontal accretion. *Journal of Geophysical Research*, 99, 12033-12055.

Larroque, C., Calassou. S., Malavieille. J., & Chanier, F., 1995. Experimental modeling of forearc

basin development during accretionary wedge growth. *Basin Research*, 7, 1255-268.

Leoni, L., Marroni, M., Sartori, F., and Tamponi, M., 1996. "Metamorphic grade in metapelites of the internal Liguride units (Northern Apennines, Italy)." *European Journal of Mineralogy*, 8, (1), 35-50.

Lester, R., McIntosh, K., Van Avendonk, J., A., Lavier, L., Liu, C-S., Wang, T.K., 2013. Crustal accretion in the Manila trench accretionary wedge at the transition from subduction to mountain-building in Taiwan, *Earth and Planetary Science Letters*, 375, 430–440.

Lewis, S.D., Hayes, D.E., 1984. A geophysical Study of the Manila Trench, Luzon, Philippines. 2. Fore Arc Basin Structural and Stratigraphic Evolution. *Journal of Geophysical Research*, 89, 9196–9214.

Lin, A.T., Yao, B., Hsu, S.-K., Liu, C.-S., Huang, C.-Y., 2009. Tectonic features of the incipient arc-continent collision zone of Taiwan: implications for seismicity. *Tectonophysics* 479, 28–42.

Liu, C.-S., Huang, I.L., Teng, L.S., 1997. Structural features off southwestern Taiwan. *Marine Geology* 137, 305–319.

Lohrmann, J., Kukowski, N., Adam, J., Oncken, O., 2003. The impact of analog material properties on the geometry, kinematics, and dynamics of convergent sand wedges. *Journal of Structural Geology*, 25, 10, p. 1691-1711. DOI: [http://doi.org/10.1016/S0191-8141\(03\)00005-1](http://doi.org/10.1016/S0191-8141(03)00005-1).

Lowe, D.R., 1982, Sediment gravity flows: II Depositional models with special reference to the deposits of high-density turbidity currents: *Journal of Sedimentary Petrology*, v. 52, no. 1, p. 279–

297.

Lucente, C.C., Pini, G.A., 2003. Anatomy and emplacement mechanism of a large sub-marine slide within the Miocene foredeep in the Northern Apennines, Italy: a field perspective. *Am J Sci* 303: 565-602.

Lundberg, N., Reed, D.L., Liu, C.-S., Lieskes Jr., J.H., 1997. Forearc-basin closure and arc accretion in the submarine suture zone south of Taiwan. *Tectonophysics*, 274, 5–24.

Malavieille, J., 1984. Modélisation expérimentale des chevauchements imbriqués: application aux chaînes de montagnes. *Bulletin de la Société Géologique de France*, 7, 129-138.

Malavieille, J., Lallemand, S.E., Dominguez, S., Deschamps, A., Lu, C-Y., Liu, C-S., Schnürle, P., and the ACT Scientific Crew, 2002. Arc-continent collision in Taiwan : New marine observations and tectonic evolution. in: Byrne, T. B. and Liu, C-S., eds., *Geology and Geophysics of an Arc-Continent collision, Taiwan. Republic of China : Bulder, Colorado, Geological Society of America Special Paper 358*, 187-211.

Malavieille, J. and Trullenque, G., 2005. Impact of forearc lithosphere subduction on forearc basins and thrust wedge deformation in SE Taiwan: insights from analogue modeling and consequences for the tectonic evolution. *Geodynamics and Environment in East Asia International Conference & 5th Taiwan-France Earth Science Symposium*, 24-29 November, 2005, Taitung, Taiwan.

Malavieille, J., Trullenque, G., 2009. Consequences of continental subduction on forearc basin and accretionary wedge deformation in SE Taiwan : Insights from analog modeling. *Tectonophysics*, 466, 377-394.

Malavieille, J., 2010. Impact of erosion, sedimentation and structural heritage on the structure and kinematics of orogenic wedges : Analog models and case studies. *GSA Today*, 20. (1), doi: 10.1130/GSATG48A.1.

Malavieille, J., Molli, G., 2014. Tectonique et géodynamique de la Corse alpine. *Géochronique* , Dossier, la Corse alpine, 132, 21-25.

Malusà, M.G., Polino, R., Zattin, M., 2009. Strain partitioning in the axial NW Alps since the Oligocene . *Tectonics* 28, 10.1029/2008TC002370

Marroni, M., 1994. Deformation path of the Internal Ligurid Units (Northern Apennines, Italy); record of shallow-level underplating in the Alpine accretionary wedge. *Memorie Della Societa Geologica Italiana* 48, Part 1, 179-194.

Marroni, M., and Pandolfi, L., 1996. The deformation history of an accreted ophiolite sequence: the Internal Liguride units (Northern Apennines, Italy). *Geodinamica Acta*, 9, 13–29.

Marroni, M., Molli, G., Montanini, A., and Tribuzio, R., 1998. The association of continental crust rocks with ophiolites in the Northern Apennines (Italy): implications for continent-ocean transition in the Western Tethys. *Tectonophysics*, 292, 43–66.

Marroni, M., and Pandolfi L., 2001. Debris flow and slide deposits at the top of the internal Liguride ophiolitic sequence, Northern Apennines, Italy : a record of frontal tectonic erosion in a fossil accretionary wedge. *Island Arc*, 10(1), 9-21.

Marroni, M., Molli, G., Montanini, A., Ottria, G., Pandolfi, L., Tribuzio, R. 2002. The external Ligurian units (Northern Apennine, Italy): from rifting to convergence of a fossil ocean-continent transition zone. *Ofioliti*, 27(2), 119-131.

Matsuda, S., and Ogawa, Y., 1993, Two-stage model of incorporation of seamount and oceanic blocks into sedimentary mélangé: Geochemical and biostratigraphic constraints in Jurassic Chichibu accretionary complex, Shikoku, Japan: *Island Arc*, v. 2, p. 7–14.

Meneghini, F., Marroni, M., Moore, J.C., Pandolfi, L., and Rowe, C.D., 2009, The processes of underthrusting and underplating in the geologic record: Structural diversity between the Franciscan Complex (California), the Kodiak Complex (Alaska) and the Internal Ligurian Units (Italy): *Geological Journal Special Issue: Dynamics in Subduction Complexes*, v. 44, no. 2, p. 126–152, doi: 10.1002/gj.114.

Mesalles, L., Mouthereau, F., Bernet, M., Chang, C-P., Lin, T-S., Fillon, C., Sengelen, X., 2014. From submarine continental accretion to arc-continent orogenic evolution: The thermal record in southern Taiwan. *GEOLOGY*, October 2014; v. 42; no. 10; p. 907–910; doi:10.1130/G35854.1

Meschede, M., Zweigel, P., Frisch, W., and Völker, D., 1999, Mélangé formation by subduction erosion: The case of the Osa mélangé in southern Costa Rica: *Terra Nova*, v. 11, p. 141–148.

Molli, G., Pandolfi, L., and Tamponi, M., 1992. “Cristallinità” di Illite e clorite nelle Unità Liguri dell’Alta Val Trebbia (Appennino Settentrionale), *Atti Soc. Tosc. Sc. Nat., Seria A*, 99, 313-326.

Molli, G. 1996. Pre-orogenic tectonic framework of the northern Apennine ophiolites. *Eclogae Geol. Helv.* 89/1, 163-180.

Molli, G., 2008. Northern Apennines-Corsica orogenic system : an updated overview. Geological Society of London, Special Publications, 298, 413-442.

Molli, G., and Malavieille, J., 2010. Orogenic processes and the Alps/Apennines geodynamic evolution: insights from Taiwan. International Journal of Earth Sciences (Geol Rundsch), DOI 10.1007/s00531-010-0598-y.

Moore, J.C., and Byrne, T., 1987, Thickening of fault zones: A mechanism of mélangé formation in accreting sediments: *Geology*, v. 15, p. 1040–1043.

Mulugeta, G., 1988. Modelling the geometry of Coulomb thrust wedges. *Journal of Structural Geology* 10 (8), 847–859.

Naylor, M., 1982. The Casanova complex of the northern Apennines: A mélangé formed on a distal passive continental margin. *Journal of Structural Geology*, 4, 1-18.

Needham, D.T., 1995, Mechanisms of mélangé formation: Examples from SW Japan and southern Scotland: *Journal of Structural Geology*, v. 17, no. 7, p. 971–985.

Ogata, K., Tinterri, R., Pini, G.A., and Mutti, E., 2012, Mass transport-related stratal disruption within sedimentary mélanges: Examples from the northern Apennines (Italy) and south-central Pyrenees (Spain): *Tectonophysics*, v. 568–569, p. 185–199. doi:10.1016/j.tecto.2011.08.021

Ogawa, Y., Mori, R., Tsunogae, T., Dilek, Y., and Harris, R., 2014, New interpretation of the Franciscan Mélangé at San Simeon coast, California: Tectonic intrusion into an accretionary prism:

International Geology Review, doi: 10.1080/00206814.2014.968813.

Orange, D.L., and Underwood, M.B., 1995, Patterns of thermal maturity as diagnostic criteria for interpretation of mélanges: *Geology*, v. 23, no. 1, p. 1144–1148.

Orr, T.O.H., Korsch, R.J., Foley, L.A., 1991. Structure of melange and associated units in the Torlesse accretionary wedge, Tararua Range, New Zealand. *New Zealand Journal of Geology and Geophysics*, 34, pp. 61–72

Osozawa, S., Morimoto, J., and Flower, F.J., 2009, ‘Block-in-matrix’ fabrics that lack shearing but possess composite cleavage planes: A sedimentary mélange origin for the Yuwan accretionary complex in the Ryukyu island arc, Japan: *Geological Society of America Bulletin*, v. 121, no. 7–8, p. 1190–1203.

Page, B.M., 1978. Franciscan mélanges compared with olistostromes of Taiwan and Italy. *Tectonophysics*, 47, 223-246.

Page, B.M., and Suppe, J., 1981. The Pliocene Lichi melange of Taiwan: Its plate-tectonic and olistostromal origin. *American Journal of Science*, Vol.281, 192-227.

Pertusati, P.C., and Horrenberger, J.C., 1975. Studio strutturale degli Scisti della Val Lavagna (Unità del Gottero, Appennino ligure). *Bollettino della Società Geologica Italiana*, 94, 1375–1436.

Platt, J.P., 2015, Origin of Franciscan blueschist-bearing melange at San Simeon, central California coast. *International Geology Review*, Vol. 57, Nos. 5-8, 843-853,

Pollock, S.G., 1989, Mélanges and olistostromes associated with ophiolitic metabasalts and their significance in Cambro-Ordovician forearc accretion in the northern Appalachians, in Horton, J.W., Jr., and Rast, N., eds., Mélanges and olistostromes of the Appalachians: Geological Society of America Special Paper 228, p. 43–64.

Principi, G., and Treves, B., 1985. Il sistema corso-appenninico come prisma d'accrezione. Riflessi sul problema generale del limite Alpi-Appennini. Memorie della Società Geologica Italiana, 28, 549–576.

Ramberg, H., 1981. Gravity, Deformation and the Earth's Crust, London. 452 pp.

Raymond, L.A., 1984. Classification of melanges. In: Melanges: Their Nature, Origin and Significance (L.A. Raymond, ed.). Geol. Soc. Am. Spec. Pap., 198, 7–20.

Reed, D.L., Lundberg, N., Liu, C.H., and Kuo, B.Y., 1992. Structural relations along the margins of the offshore Taiwan accretionary wedge: implications for accretion and crustal kinematics. Acta Geologica Taiwanica 30, 105–122.

Remitti, F., Vannucchi, P., Bettelli, G., Fantoni, L., Panini, F., and Vescovi, P., 2011. Tectonic and sedimentary evolution of the frontal part of an ancient subduction complex at the transition between accretion and erosion: The case of the Ligurina wedge of the northern Apennines. Geological Society of America Bulletin, 123 (1-2), 51-70, doi : 10.1130/B30065.1

Roure, F., Casero, P., and Vially, R., 1991, Growth processes and melange formation in the southern Apennines accretionary wedge: Earth and Planetary Science Letters, v. 102, p. 395–412.

Sakai, H., 1981, Olistostrome and sedimentary mélange of the Shimanto Terrane in the southern part of the Muroto Peninsula, Shikoku: Scientific Reports, Department of Geology, Kyushu University 14, p. 81–101.

Saleeby, J., 1984, Tectonic significance of serpentinite mobility and ophiolitic melange, in Raymond, L.A., ed., *Melanges: Their nature, origin, and significance*: Geological Society of America Special Paper 198, p. 153–168.

Schellart, W.P., 2000. Shear test results for cohesion and friction coefficients for different granular materials: scaling implications for their usage in analogue modelling. *Tectonophysics* 324 (1–2), 1–16.

Silver, E.A., and Beutner, E.C., 1980, *Melanges: Geology*, v. 8, p. 32–34.

Simoès, M., Avouac, J.P., Beyssac, O., Goffe, B., Farley, K.A., Chen, Y.-G., 2007. Mountain building in Taiwan: A thermokinematic model. *Journal of Geophysical Research* 112, B11405. doi:10.1029/2006JB004824.

Steen, O., and Andreson, A., 1997, Deformational structures associated with gravitational block gliding: Examples from sedimentary olistoliths in the Kalvag Mélange, western Norway: *American Journal of Science*, v. 297, p. 56–97, doi: 10.2475 /ajs .297 .1 .56 .

Summerfield, M.A., and Hulton, N.J., 1994. Natural controls of fluvial denudation rates in major drainage basins. *J. Geophys. Res.*, 99, 7, 13871-13883.

Suppe, J., 1984. Kinematics of arc-continent collision, flipping of subduction, and back-arc

spreading near Taiwan. *Memoir of the Geological Society of China* 6, 21–33.

Suppe, J., Lan, C.Y., Hendel, E.M., and Liou, J.G., 1977, Paleogeographic interpretation of red shales within the East Taiwan Ophiolite: *Petroleum Geology Taiwan*, 14, 109-120.

Suppe, J., and Liou, J.G., 1979. Tectonics of the Lichi Mélange and East Taiwan Ophiolite. *Memoir of the Geological Society of China*, N°. 3, PP. 147-153.

Talbot, C.J., and von Brunn, V., 1989, Melanges, intrusive and extrusive sediments, and hydraulic arcs: *Geology*, v. 17, p. 446–448.

Treves, B., 1984 Orogenic belts as accretionary prisms: the example of the Northern Apennines. *Ofioliti*, 9, 577–618.

Ukar, E., 2012, Tectonic significance of low-temperature blueschist blocks in the Franciscan mélange at San Simeon, California. *Tectonophysics* 568–569 (2012) 154–169.

Ukar, E., and Cloos, M., 2013, Actinolite rinds on low-T mafic blueschist blocks in the Franciscan shale-matrix mélange near San Simeon: Implications for metasomatism and tectonic history: *Earth and Planetary Science Letters*, v. 377–378, p. 155–168, doi: 10.1016/j.epsl.2013.06.038 .

Ukar, E., and Cloos, M., 2015, Magmatic origin of low-T mafic blueschist and greenstone blocks from the Franciscan mélange, San Simeon, California. *Lithos*, Volume 230, 1 August 2015, Pages 17–29, doi:10.1016/j.lithos.2015.05.002

Van Puybroeck, N., Michel, R., Binet, R., Avouac, J.-P. and Taboury, J., 2000. Measuring earthquakes from optical satellite image. *Applied Optics*, 39.

Von Huene, R., Ranero, C., Vannucchi, P., 2004. Generic model of subduction erosion. *Geology*; v. 32; no. 10; p. 913–916; doi: 10.1130/G20563.1

Wakabayashi, J., 2011a. Subducted sedimentary serpentinite mélanges: Record of multiple burial-exhumation cycles and subduction erosion, *Tectonophysics*, doi: 10.1016/j.tecto.2011.11.006.

Wakabayashi, J., 2011b, Mélanges of the Franciscan complex, California: Diverse structural settings, evidence for sedimentary mixing, and their connection to subduction processes, in Wakabayashi, J., and Dilek, Y., eds., *Mélanges: Processes of Formation and Societal Significance: Geological Society of America Special Paper 480*, p. 117–141.

Yilmaz, P.O., and Maxwell, J.C., 1984, An example of an obduction melange: The Alakir Çay unit, Antalya Complex, southwest Turkey, in Raymond, L.A., ed., *Mélanges: Their nature, origin, and significance: Geological Society of America Special Paper 198*, p. 139–152.